

AD743992

# RESEARCH AND DEVELOPMENT OF RARE EARTH-TRANSITION METAL ALLOYS AS PERMANENT-MAGNET MATERIALS

A. E. Ray and K. J. Strnat

Research Institute  
University of Dayton

Sponsored by

Advanced Research Projects Agency  
ARPA Order No. 1617

TECHNICAL REPORT AFML-TR-72-99

April 1972

Approved for public release;  
distribution unlimited.



The views and conclusions contained in this document are those of the authors and should not be interpreted as necessarily representing the official policies, either expressed or implied, of the advanced Research Projects Agency or the U.S. Government.

Air Force Materials Laboratory  
Air Force Systems Command  
Wright-Patterson Air Force Base, Ohio

Reproduced by  
NATIONAL TECHNICAL  
INFORMATION SERVICE  
U S Department of Commerce

65  
R

## NOTICE

When Government drawings, specifications, or other data are used for any purpose other than in connection with a definitely related Government procurement operation, the United States Government thereby incurs no responsibility nor any obligation whatsoever; and the fact that the Government may have formulated, furnished, or in any way supplied the said drawings, specifications, or other data, is not to be regarded by implication or otherwise as in any manner licensing the holder or any other person or corporation, or conveying any rights or permission to manufacture, use, or sell any patented invention that may in any way be related thereto.

ADDITIONAL BY		
DDO	WHITE SECTION	<input checked="checked" type="checkbox"/>
DDO	BUFF SECTION	<input type="checkbox"/>
UNANNOUNCED		<input type="checkbox"/>
JUSTIFICATION		
BY		
DISTRIBUTION/AVAILABILITY CODES		
DIST.	AVAIL.	and/or SPECIAL
A		

Copies of this report should not be returned unless return is required by security considerations, contractual obligations, or notice on a specific document.

## DOCUMENT CONTROL DATA - R&amp;D

(Security classification of title, body of abstract and indexing annotation must be entered when the overall report is classified)

## 1. ORIGINATING ACTIVITY (Corporate author)

University of Dayton  
Research Institute  
Dayton, Ohio 45409

## 2a. REPORT SECURITY CLASSIFICATION

Unclassified

## 2b. GROUP

## 3. REPORT TITLE

RESEARCH AND DEVELOPMENT OF RARE EARTH-TRANSITION  
METAL ALLOYS AS PERMANENT-MAGNET MATERIALS

## 4. DESCRIPTIVE NOTES (Type of report and inclusive dates)

Semiannual Interim Technical Report: 1 July 1971 - 31 December 1971

## 5. AUTHOR(S) (Last name, first name, initial)

Ray, Alden E.  
Strnat, Karl J.

## 6. REPORT DATE

April 1972

## 7a. TOTAL NO. OF PAGES

51

## 7b. NO. OF REFS

19

## 8a. CONTRACT OR GRANT NO.

F33615-70-C-1625

## b. PROJECT NO.

7371

## c.

Task No. 73103

## d.

## 9a. ORIGINATOR'S REPORT NUMBER(S)

UDRI-TR-72-24

## 9b. OTHER REPORT NO(S) (Any other numbers that may be assigned this report)

AFML-TR-72-99

## 10. AVAILABILITY/LIMITATION NOTICES

Approved for public release; distribution unlimited.

## 11. SUPPLEMENTARY NOTES

## 12. SPONSORING MILITARY ACTIVITY

Air Force Materials Laboratory  
Wright-Patterson AFB, Ohio 45433

## 13. ABSTRACT

Mixed intermetallic phases of the type  $R_2(Co_{1-x}Fe_x)_{17}$  with  $R=Ce, Pr, Nd, Sm, Y$ , and MM (Ce-rich mischmetal) are being studied as potential permanent magnet materials. Except for  $R=Nd$ , all show ranges of  $x$  in which the crystallographic  $c$ -axis is the easy axis of magnetization. During the present period, these ranges have been more precisely defined and quantitative measurements of the saturation magnetization and crystal anisotropy constants initiated. It is concluded that some of these alloys are indeed promising candidate materials for improved rare earth-cobalt magnets.

The composition dependence of selected metallurgical and magnetic properties of phases of the type  $Nd_{1-x}R_xCo_{17}$ , where  $R=Ce, Pr$ , and  $Y$ , are under investigation. Peritectic melting temperatures, lattice constants, Curie temperatures, and saturation-magnetization measurements are reported. Single crystals of several of the mixed phases have been prepared and saturation magnetization and room-temperature anisotropy measurements on these have been initiated.

New cobalt-rich intermetallic phases have been found in three binary rare earth-cobalt alloy systems. Single phase alloys of  $Ce_5Co_{19}$ ,  $Pr_5Co_{19}$ , and  $Nd_5Co_{19}$  have been prepared. Lattice constants for the rhombohedral forms of these phases were also measured and found to lie between those of the corresponding  $RCo_5$  and  $R_2Co_7$ .

Successful attempts were made to enhance the intrinsic coercive force of  $Sm_2Co_{17}$  by sintering with a Sm-Co addition. Sintering of compacts made from  $Sm_2Co_{17}$  powder of  $M_H < 1000$  Oe with Sm60/Co40 yielded magnets with coercive forces of up to 9600 Oe.

14. KEY WORDS	LINK A		LINK B		LINK C	
	ROLE	WT	ROLE	WT	ROLE	WT
Magnetic Materials Magnetic Properties Permanent Magnets Rare Earth Alloys Intermetallic Compounds						

### INSTRUCTIONS

**1. ORIGINATING ACTIVITY:** Enter the name and address of the contractor, subcontractor, grantee, Department of Defense activity or other organization (corporate author) issuing the report.

**2a. REPORT SECURITY CLASSIFICATION:** Enter the overall security classification of the report. Indicate whether "Restricted Data" is included. Marking is to be in accordance with appropriate security regulations.

**2b. GROUP:** Automatic downgrading is specified in DoD Directive 5200.10 and Armed Forces Industrial Manual. Enter the group number. Also, when applicable, show that optional markings have been used for Group 3 and Group 4 as authorized.

**3. REPORT TITLE:** Enter the complete report title in all capital letters. Titles in all cases should be unclassified. If a meaningful title cannot be selected without classification, show title classification in all capitals in parentheses immediately following the title.

**4. DESCRIPTIVE NOTES:** If appropriate, enter the type of report, e.g., interim, progress, summary, annual, or final. Give the inclusive dates when a specific reporting period is covered.

**5. AUTHOR(S):** Enter the name(s) of author(s) as shown on or in the report. Enter last name, first name, middle initial. If military, show rank and branch of service. The name of the principal author is an absolute minimum requirement.

**6. REPORT DATE:** Enter the date of the report as day, month, year; or month, year. If more than one date appears on the report, use date of publication.

**7a. TOTAL NUMBER OF PAGES:** The total page count should follow normal pagination procedures, i.e., enter the number of pages containing information.

**7b. NUMBER OF REFERENCES:** Enter the total number of references cited in the report.

**8a. CONTRACT OR GRANT NUMBER:** If appropriate, enter the applicable number of the contract or grant under which the report was written.

**8b, 8c, & 8d. PROJECT NUMBER:** Enter the appropriate military department identification, such as project number, subproject number, system numbers, task number, etc.

**9a. ORIGINATOR'S REPORT NUMBER(S):** Enter the official report number by which the document will be identified and controlled by the originating activity. This number must be unique to this report.

**9b. OTHER REPORT NUMBER(S):** If the report has been assigned any other report numbers (either by the originator or by the sponsor), also enter this number(s).

**10. AVAILABILITY/LIMITATION NOTICES:** Enter any limitations on further dissemination of the report, other than those

imposed by security classification, using standard statements such as:

- (1) "Qualified requesters may obtain copies of this report from DDC."
- (2) "Foreign announcement and dissemination of this report by DDC is not authorized."
- (3) "U. S. Government agencies may obtain copies of this report directly from DDC. Other qualified DDC users shall request through \_\_\_\_\_."
- (4) "U. S. military agencies may obtain copies of this report directly from DDC. Other qualified users shall request through \_\_\_\_\_."
- (5) "All distribution of this report is controlled. Qualified DDC users shall request through \_\_\_\_\_."

If the report has been furnished to the Office of Technical Services, Department of Commerce, for sale to the public, indicate this fact and enter the price, if known.

**11. SUPPLEMENTARY NOTES:** Use for additional explanatory notes.

**12. SPONSORING MILITARY ACTIVITY:** Enter the name of the departmental project office or laboratory sponsoring (paying for) the research and development. Include address.

**13. ABSTRACT:** Enter an abstract giving a brief and factual summary of the document indicative of the report, even though it may also appear elsewhere in the body of the technical report. If additional space is required, a continuation sheet shall be attached.

It is highly desirable that the abstract of classified reports be unclassified. Each paragraph of the abstract shall end with an indication of the military security classification of the information in the paragraph, represented as (TS), (S), (C), or (U).

There is no limitation on the length of the abstract. However, the suggested length is from 150 to 225 words.

**14. KEY WORDS:** Key words are technically meaningful terms or short phrases that characterize a report and may be used as index entries for cataloging the report. Key words must be selected so that no security classification is required. Identifiers, such as equipment model designation, trade name, military project code name, geographic location, may be used as key words but will be followed by an indication of technical context. The assignment of links, rules, and weights is optional.

1a

RESEARCH AND DEVELOPMENT OF RARE EARTH-TRANSITION  
METAL ALLOYS AS PERMANENT-MAGNET MATERIALS

By:

Dr. Alden E. Ray and Dr. Karl J. Strnat, Principal Investigators  
University of Dayton, Research Institute and Electrical Engineering Dept.  
300 College Park Ave., Dayton, Ohio 45409  
Tel. Numbers: (513) 229-3527 and (513) 229-3611

Sponsored by:

Advanced Research Projects Agency  
ARPA Order No. 1617

Program Code No. OD10  
Contract effective date: 30 June 1970  
Expiration date: 30 June 1973  
Amount of contract: \$525,012

Submitted to:

Air Force Materials Laboratory, AFSC, USAF  
Project Scientist: Mr. Donald J. Evans, LPE Tel. (513) 255-4474

Details of illustrations in  
this document may be better  
studied on microfiche

Approved for public release;  
distribution unlimited.

*IR*

*II's*

## FOREWORD

The research described in this report is part of the contractual research program of the Materials Physics Division, Air Force Materials Laboratory. It was performed by the authors at the University of Dayton, Dayton, Ohio 45409, and was sponsored by the Advanced Research Projects Agency, ARPA Order No. 1617, Program Code No. OD10. The contract is administered under Project No. 7371, Task No. 737103, by the Air Force Materials Laboratory, Air Force Systems Command, Wright-Patterson Air Force Base, Ohio. The work was performed under contract F33615-70-C-1625, project scientist, Mr. Donald Evans (AFML/LPE/513-255-4474).

The participants in this research were Adolf Biermann, John Geis, Richard Harmer, Michael Hartings, Andrew Kraus, Robert Leasure, Herbert Mildrum, Shukdor Rashidi, Alden Ray, Jacques Schweizer, Charles Shanley, Karl Strnat, James Tsui, and David Walsh.

This report covers research conducted between 1 July 1971 and 31 December 1971. The report was submitted by the authors in April 1972.

Publication of this report does not constitute Air Force approval of the report's findings and conclusions. It is published only for the exchange and stimulation of ideas.

  
CHARLES E. EHRENFRIED

Major, USAF

Chief, Electromagnetic Materials Branch  
Materials Physics Division  
Air Force Materials Laboratory

## ABSTRACT

Mixed intermetallic phases of the type  $R_2(Co_{1-x}Fe_x)_{17}$  with  $R = Ce, Pr, Nd, Sm, Y,$  and MM (Ce-rich mischmetal) are being studied as potential permanent magnet materials. Except for  $R = Nd$ , all show ranges of  $x$  in which the crystallographic  $c$ -axis is the easy axis of magnetization. During the present period, these ranges have been more precisely defined and quantitative measurements of the saturation magnetization and crystal anisotropy constants initiated. It is concluded that some of these alloys are indeed promising candidate materials for improved rare earth-cobalt magnets.

The composition dependence of selected metallurgical and magnetic properties of phases of the type  $Nd_{1-x}R_xCo_5$ , where  $R = Ce, Pr,$  and  $Y$ , are under investigation. Peritectic melting temperatures, lattice constants, Curie temperatures, and saturation-magnetization measurements are reported. Single crystals of several of the mixed phases have been prepared and saturation magnetization and room-temperature anisotropy measurements on these have been initiated.

New cobalt-rich intermetallic phases have been found in three binary rare earth-cobalt alloy systems. Single phase alloys of  $Ce_5Co_{19}, Pr_5Co_{19},$  and  $Nd_5Co_{19}$  have been prepared. Lattice constants for the rhombohedral forms of these phases are reported. The Curie temperatures of these phases were also measured and found to lie between those of the corresponding  $RCO_5$  and  $R_2Co_7$ .

Successful attempts were made to enhance the intrinsic coercive force of milled  $\text{RCo}_5$  alloys with  $\text{R} = \text{Nd}$  and  $\text{Di}$  (didymium) by sintering with  $\text{Pr-Co}$  and  $\text{Sm-Co}$  additions. Sintering  $\text{NdCo}_5$  powders with as-ground coercive force of  $H_c^M = 190$  Oe with  $\text{Pr-Co}$  additive raised the coercive force to  $H_c^M = 4000$  Oe; the coercive force of  $\text{DiCo}_5$  could be increased from 130 Oe to  $H_c^M = 10,280$  Oe. Sintering of compacts made from  $\text{Sm}_2\text{Co}_{17}$  powder of  $H_c^M < 1000$  Oe with  $\text{Sm60/Co40}$  yielded magnets with coercive forces of up to 9600 Oe.

# TABLE OF CONTENTS

<u>Section</u>		<u>Page</u>
I	MAGNETIC PROPERTIES OF $R_2(Co, Fe)_{17}$ PHASES	
	A. INTRODUCTION .....	1
	B. EASY DIRECTIONS OF MAGNETIZATION IN TERNARY $R_2(Co, Fe)_{17}$ PHASES .....	3
	C. MAGNETIC TRANSITION TEMPERATURES OF $R_2(Co, Fe)_{17}$ PHASES .....	4
	D. MAGNETIZATION MEASUREMENTS .....	18
	E. THE PROSPECTS FOR $R_2(Co, Fe)_{17}$ MAGNETS....	23
II	METALLURGICAL AND MAGNETIC PROPERTIES OF SOME $Nd_{1-x}R_xCo_5$ ALLOYS	
	A. INTRODUCTION .....	30
	B. ALLOY PREPARATION .....	30
	C. THERMAL ANALYSIS .....	31
	D. LATTICE CONSTANTS.....	31
	E. PREPARATION OF SINGLE CRYSTALS.....	35
	F. MAGNETIC CURIE TEMPERATURE MEASUREMENTS .....	36
III	METALLURGY OF THE $R_5Co_{19}$ PHASES	
	A. INTRODUCTION .....	46
	B. PREPARATION OF THE ALLOYS .....	46
	C. RESULTS .....	47
	REFERENCES.....	50

## LIST OF ILLUSTRATIONS

<u>Figure</u>		<u>Page</u>
1.	Magnetic symmetry of $R_2(\text{Co}_{1-x}\text{Fe}_x)_{17}$ phases. Shaded areas indicate the range of $x$ in which the crystallographic $c$ -axis is the direction of easy magnetization. ....	5
2.	TMA spectrum of $\text{Y}_2(\text{Co}_{.9}\text{Fe}_{.1})_{17}$ alloy. Solid line is the heating curve; dashed line is the cooling curve. ....	7
3.	$T_c$ vs. $x$ for $\text{Y}_2(\text{Co}_{1-x}\text{Fe}_x)_{17}$ ....	9
4.	$T_c$ vs. $x$ for $\text{Sm}_2(\text{Co}_{1-x}\text{Fe}_x)_{17}$ ....	11
5.	TMA spectrum of $\text{Sm}_2(\text{Co}_{.4}\text{Fe}_{.6})_{17}$ alloy. Solid line is the heating curve; dashed line is the cooling curve. ....	12
6.	TMA spectrum of $\text{Ce}_2(\text{Co}_{.4}\text{Fe}_{.6})_{17}$ alloy. Solid line is the heating curve; dashed line is the cooling curve. ....	14
7.	$T_c$ vs. $x$ and temperatures of other irregularities in the TMA spectra of $\text{Ce}_2(\text{Co}_{1-x}\text{Fe}_x)_{17}$ phases. ....	15
8.	Easy-axis and hard-axis magnetization curves measured on oriented powders of three $\text{Sm}_2(\text{Co}_{1-x}\text{Fe}_x)_{17}$ alloys. ....	20
9.	Magnetization curves measured on oriented powders of three $\text{Pr}_2(\text{Co}_{1-x}\text{Fe}_x)_{17}$ alloys. ....	21
10.	Magnetization curves measured on oriented powders of three $\text{MM}_2(\text{Co}_{1-x}\text{Fe}_x)_{17}$ alloys. ....	22

# LIST OF ILLUSTRATIONS

<u>Figure</u>		<u>Page</u>
11.	Saturation induction values at room temperature for the compounds $R_2Co_{17}$ , $R_2Fe_{17}$ and $RCo_5$ . . . . .	25
12.	Composition dependence of the room-temperature saturation in the systems Co-Fe and $Y_2Co_{17} - Y_2Fe_{17}$ . . . . .	27
13.	Theoretically possible energy products for magnets made from selected $R_2(Co, Fe)_{17}$ phases compared to best experimental and theoretical values for other magnet types. . . . .	29
14.	Melting and peritectic temperatures for $Nd_{1-x}R_xCo_5$ alloys. . . . .	32
15.	Slightly rare earth rich $Nd_{0.5}Ce_{0.5}Co_5$ alloy (AR-978) as-cast. The gray phase is either an $R_5Co_{19}$ or $R_2Co_7$ phase. Bright field illumination. . . .	37
16.	$Nd_{0.5}Ce_{0.5}Co_5$ alloy (AR-978) homogenized for 168 hours at $1170^\circ C$ . Extensive grain growth is evident. Polarized light was employed to reveal the magnetic domain pattern within the large grains. . . . .	37
17.	Laue photograph of a $PrCo_5$ crystal oriented with its c-axis parallel to the x-ray beam. The diffraction spots correspond closely with the size and shape of the crystal fragment. . . . .	38
18.	Results of Curie point measurements by TMA in the alloy system $Nd_{1-x}Ce_xCo_5$ . . . . .	40
19.	Results of Curie point measurements by TMA in the alloy system $NdCo_5 - PrCo_5$ . . . . .	43

# LIST OF TABLES

<u>Table</u>		<u>Page</u>
I.	List of $R_2(\text{Co, Fe})_{17}$ Alloys Thermomagnetically Analyzed .....	16
II.	Tentative Results of Saturation Magnetization Measurements on $R_2(\text{Co}_{1-x}\text{Fe}_x)_{17}$ Phases .....	18
III.	Thermal Events Observed by DTA for Some Binary and Ternary $\text{RCo}_5$ Alloys .....	33
IV.	Lattice Constants for $\text{Nd}_{1-x}\text{Ce}_x\text{Co}_5$ and $\text{Nd}_{1-x}\text{Pr}_x\text{Co}_5$ Phases .....	34
V.	List of $\text{RCo}_5$ Alloys Thermomagnetically Analyzed .....	45
VI.	Lattice Constants, Curie Temperatures, and Peritectic Temperatures for $\text{Ce}_5\text{Co}_{19}$ , $\text{Pr}_5\text{Co}_{19}$ , and $\text{Nd}_5\text{Co}_{19}$ .....	48
VII.	Powder X-Ray Diffraction Patterns for $\text{Ce}_5\text{Co}_{19}$ , $\text{Pr}_5\text{Co}_{19}$ , and $\text{Nd}_5\text{Co}_{19}$ .....	49

MAGNETIC PROPERTIES OF  $R_2(\text{Co, Fe})_{17}$  PHASES

## A. INTRODUCTION

Mixed intermetallic phases of the type  $R_2(\text{Co}_{1-x}\text{Fe}_x)_{17}$  are being studied as possible high-energy, high coercive-force permanent magnet materials. For a ferromagnetic substance to qualify for this application, three basic magnetic properties must be favorable: saturation magnetization and Curie temperature must be high, and the magnetocrystalline anisotropy must be such that, ideally, a single direction in the crystal lattice is strongly preferred by the spontaneous magnetization vector. The intermetallic compounds of the type  $\text{RCo}_5$  between rare earth metals (symbol R) and cobalt meet these conditions quite well. The intermetallic phases,  $R_2\text{Co}_{17}$ , have even higher saturation values and Curie points.<sup>(1,2)</sup> However, the first compound in this class on which room temperature anisotropy measurements were made,  $\text{Y}_2\text{Co}_{17}$ , has a much lower anisotropy constant,  $K_1$ , than the  $\text{RCo}_5$  phases. Moreover,  $K_1$  is negative,<sup>(3,4)</sup> so that the c-axis is magnetically hard and the easy directions are in the basal plane. In view of this discouraging early result and because of the exciting promise of the  $\text{RCo}_5$  phases, further study of the  $R_2\text{Co}_{17}$  compounds was delayed for several years. It did become known that  $\text{Sm}_2\text{Co}_{17}$  has the favorable easy-axis anisotropy,<sup>(5)</sup> but its anisotropy field is only about 25% of that of  $\text{SmCo}_5$ .

In contrast to the  $\text{RCo}_5$  phases, which have no " $\text{RFe}_5$ " counterparts, there is a family of rare earth-iron compounds of the type  $R_2\text{Fe}_{17}$ .<sup>(6)</sup> While

these have higher absolute saturation moments than their cobalt equivalents, they have lower Curie points.<sup>(7)</sup> The  $R_2Co_{17}$  and  $R_2Fe_{17}$  phases of most of the rare earth elements were recently investigated<sup>(8)</sup> to find if any, other than  $Sm_2Co_{17}$ , had the desired magnetic symmetry. It was found that all of the  $R_2Fe_{17}$  phases and most of the  $R_2Co_{17}$  phases showed easy-basal-plane anisotropy. Only the  $R_2Co_{17}$  phases with  $R = Sm, Er, \text{ and } Tm$  were observed to have the c-axis as the easy direction of magnetization.

We were reasonably confident on the basis of theoretical considerations that by preparing ternary phases of the type  $R_2(Co, Fe)_{17}$ , we could achieve a favorable compromise between the high saturation magnetizations of the  $R_2Fe_{17}$  and the high Curie temperatures of the  $R_2Co_{17}$  phases. It was also recognized that the key property for permanent magnet applications is a large, uniaxial magnetocrystalline anisotropy and that the mixing of cobalt and iron in the T-sites of  $R_2T_{17}$  compounds in alloying combinations of the type  $R_2(Co_{1-x}Fe_x)_{17}$  should strongly influence the magnetocrystalline anisotropy. We also thought that this mixing of Fe and Co may induce a favorable magnetic symmetry in these phases even where it does not exist for the terminal phases of the quasi-binary systems,  $R_2Co_{17}$  and  $R_2Fe_{17}$ .

Initial screening tests were concentrated on the Curie temperatures and magnetic symmetries. The results of these tests<sup>(9)</sup> must be termed extremely encouraging. Our measurements show that while the Curie points are monotonically lowered by the substitution of iron for cobalt, the absolute Curie temperatures remain very high, above  $600^\circ C$ , for iron substitution

up to 50% or more. Moreover, of the six quasi-binary  $R_2Co_{17}-R_2Fe_{17}$  systems with  $R = Ce, Pr, Nd, Sm, Y,$  and  $MM$  studied, all except  $R = Nd$  display wide composition ranges in which the  $c$ -axis indeed becomes the easy direction of magnetization.

During this reporting period, we have defined more precisely the compositional ranges in which this easy- $c$ -axis symmetry prevails and have conducted quantitative measurements of the saturation magnetization and crystal anisotropy constants for alloys lying in these ranges.

B. EASY DIRECTIONS OF MAGNETIZATION IN TERNARY  
 $R_2(Co, Fe)_{17}$  PHASES (Shanley, Harmer, Ray)

The alloys were prepared by arc melting of the elements followed by vacuum annealing below the peritectic or melting temperatures, as previously described.<sup>(9)</sup> The crystal axis of easy magnetization was determined from x-ray diffraction measurements on powders aligned in a magnetic field. Powders of -200 mesh ( $<78 \mu m$ ) were prepared by mortar grinding and sifting. The particles were premagnetized in a field of 26 kOe, mixed with epoxy resin, and placed in a 6 kOe field to orient the particles while the binder hardened. The needle-shaped samples so produced were placed in a Weissenberg camera and rotating-crystal diffraction patterns were obtained. Vanadium-filtered  $CrK_{\alpha}$  radiation was employed. The patterns obtained are typical of those of a strongly textured sample. The crystallographic nature of the axis which preferentially aligned with the applied field was determined by qualitative evaluation of this texture.

The crystal-anisotropy studies revealed that the easy-axis symmetry of  $\text{Sm}_2(\text{Co}_{1-x}\text{Fe}_x)_{17}$  alloys is retained up to  $x = 0.5$ . When more than half of the cobalt is replaced by iron, the easy direction changes from the c-axis to the basal plane. Substitution of even small amounts of Fe for Co in the systems in which the rare earth is either Ce, Pr, or Y brings about easy c-axis behavior, which again prevails until about 50% of the cobalt is replaced. (In the Pr-system it persists to  $x = 0.6$ .) Because of its potential interest in the commercial production of inexpensive magnets, cerium-rich mischmetal (MM) was also investigated. Here the easy c-axis range extends from  $x = 0.1$  to  $x = 0.45$ . These results are schematically summarized in Figure 1. Of the six quasi-binary systems investigated, only that in which the rare earth is neodymium exhibits easy-basal-plane symmetry over the entire range from  $x = 0$  to 1.0.

#### C. MAGNETIC TRANSITION TEMPERATURES OF $\text{R}_2(\text{Co}, \text{Fe})_{17}$ PHASES (Hartings, Mildrum, Strnat)

We have previously reported Curie temperatures for the six  $\text{R}_2(\text{Co}_{1-x}\text{Fe}_x)_{17}$  systems with  $\text{R} = \text{Y}, \text{Ce}, \text{Pr}, \text{Nd}, \text{Sm}$  and MM determined mainly by differential thermal analysis.<sup>(9)</sup> During heating or cooling through the Curie temperature, a minor thermal event occurs. If one knows where to look for it, as one does in these systems because of the expected systematic composition dependence of any of the properties, one can determine the temperature of magnetic ordering from the first deviation of the cooling curve from a smooth line.  $T_c$  can be precisely located only on the cooling

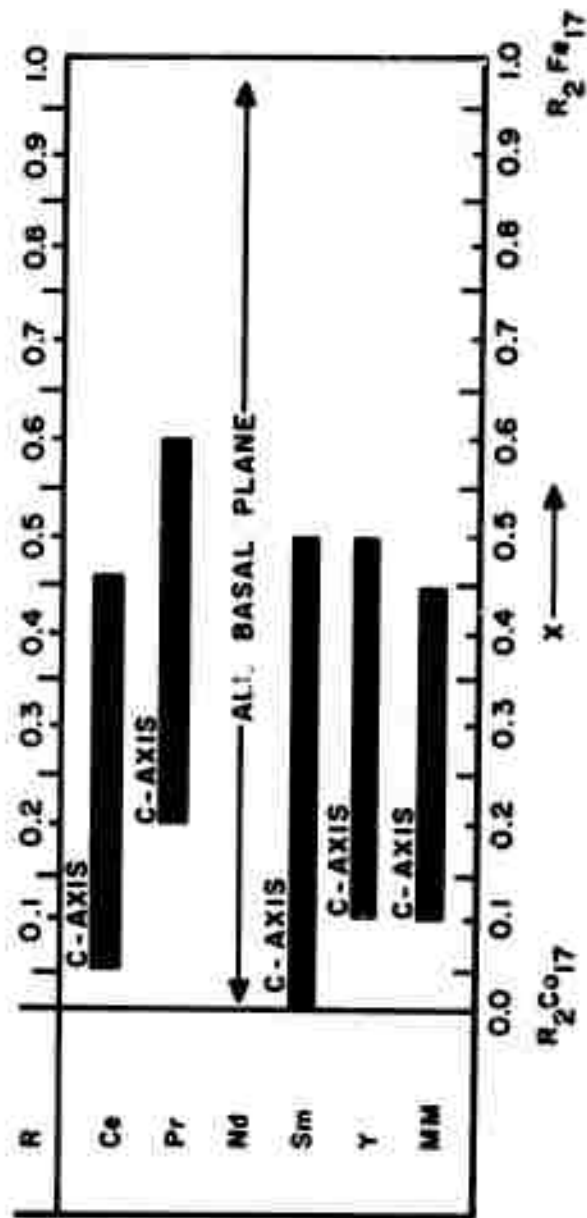


Figure 1. Magnetic symmetry of  $R_2(\text{Co}_{1-x}\text{Fe})_{17}$  phases. Shaded areas indicate the range of  $x$  in which the crystallographic c-axis is the direction of easy magnetization.

curve. Due to the second-order nature of most magnetic transitions, DTA heating curves are rather useless in this analysis. The temperature control and measurement system in our DTA apparatus permits the reliable determination of magnetic transition temperatures in this manner only above  $400^{\circ}\text{C}$ . To supplement the DTA results and to extend them to  $x = 1$ , where  $T_c < 400^{\circ}\text{C}$ , we had previously performed and included in the last semiannual report several thermomagnetic analyses (TMA) on iron-rich alloys in the Ce-Co-Fe and Sm-Co-Fe alloy systems. The TMA apparatus and the measurement technique were also described in that report.<sup>(9)</sup> A "TMA spectrum" is a plot of the measured induction voltage (closely related to the initial permeability,  $\mu_i$ ) as a function of temperature.

In the period covered by the present report, TMA of this kind were performed from room temperature upwards on all the alloys available in the  $R_2(\text{Co}_{1-x}\text{Fe}_x)_{17}$  systems where R is samarium or cerium, and from  $x = 0$  to 0.6 in the system with R = yttrium.

The TMA spectra of the Y-Co-Fe alloys are the simplest. Figure 2 illustrates the behavior of  $\text{Y}_2(\text{Co}_{.9}\text{Fe}_{.1})_{17}$  which is qualitatively typical for all other alloys in this system. The curve exhibits a pronounced Hopkinson maximum followed by an abrupt drop of the curve on the high-temperature side, and a minor second step at a slightly higher temperature. The shape of the major Hopkinson peak is characteristic of a normal, second-order Curie transition such as that of the simple ferromagnets iron, cobalt or nickel. The curves are very similar on heating and cooling and show no

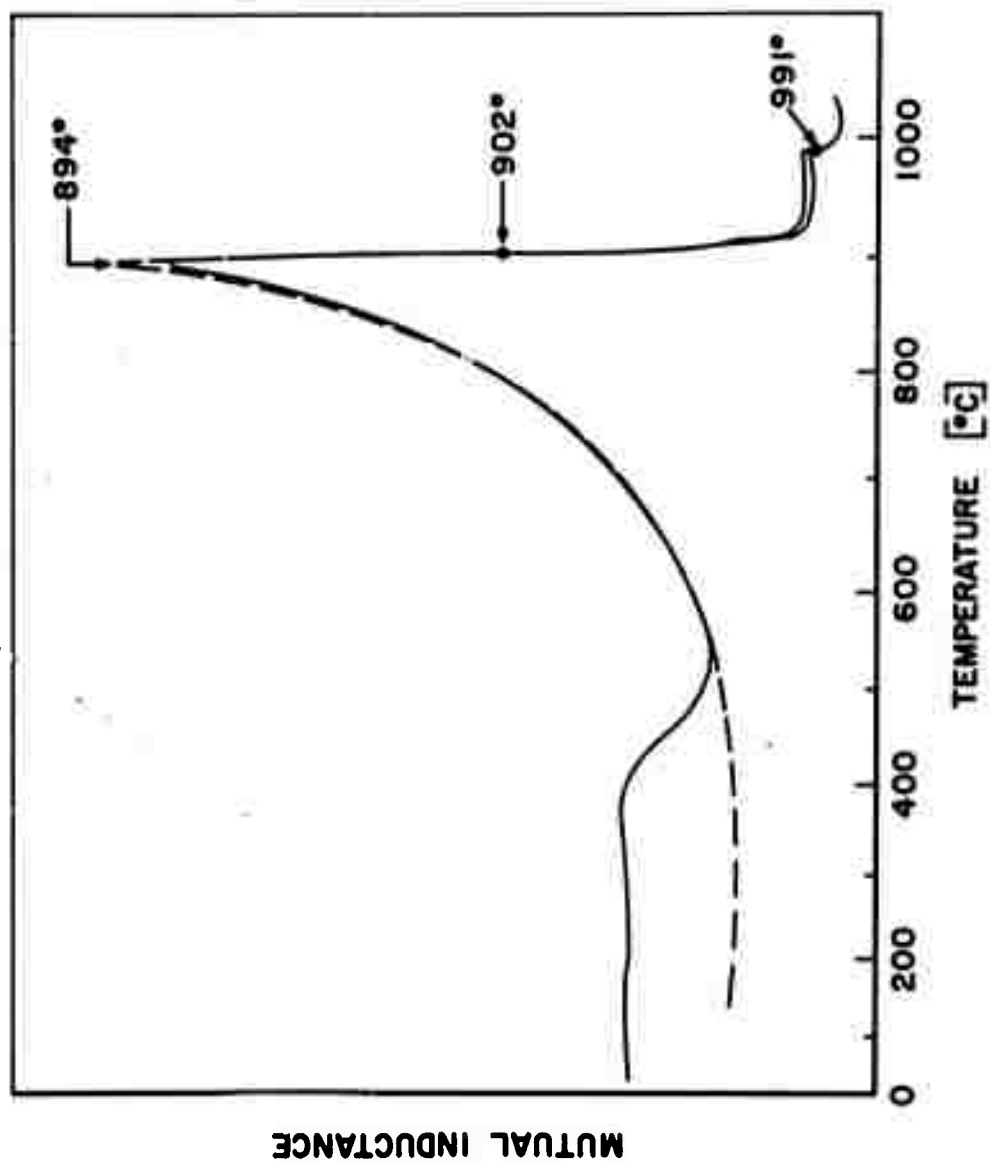


Figure 2. TMA spectrum of  $Y_2(Co_{0.9}Fe_{0.1})_{17}$  alloy. Solid line is the heating curve; dashed line is the cooling curve.

thermal hysteresis. Repeated cycling consistently gives the same results. In analyzing the curves, we took the point of inflection on the steep slope above the major peak as indicator of the Curie temperature. The results obtained to date are summarized in Figure 3. The  $T_c$  data so obtained correspond very closely to those previously determined by DTA.

The position of the minor step has a composition dependence which is quite different from that of the major peak. The step lies above  $T_c$  for  $x = 0$  and  $0.1$ , coincides with it for  $x = 0.2$ , and then drops rapidly with increasing  $x$  to  $230^\circ\text{C}$  for  $x = 0.5$ . No second step was observed for  $x = 0.6$ . By extrapolation one might expect it to occur near  $-200^\circ\text{C}$ , but we have not yet performed TMA below room temperature. For  $\text{Y}_2\text{Co}_{17}$  ( $x = 0$ ), the second step coincides with the Curie temperature of pure Cobalt. (The  $\text{Y}_2\text{Co}_{17}$  alloy was not analyzed as part of the present investigation. The data used is from previous work of J. C. Olson.)<sup>(10)</sup> It had been shown that the " $\text{Y}_2\text{Co}_{17}$ " alloy on which the TMA was performed contained a small amount of cobalt as a second phase. This suggests that the secondary "TMA event" in the  $\text{Y}_2(\text{Co}, \text{Fe})_{17}$  alloys may also be attributable to a second-phase impurity which is substantially a cobalt-iron alloy. The "event" would then be the Curie temperature of the  $\gamma$ -modification of the Co-Fe binary phase. If this were indeed the case, it would follow that the Fe:Co ratio is greater in this impurity phase than in the main phase. Furthermore, the magnetic results would suggest that the small quantities of yttrium that can be in solid solution in the Co-Fe are capable of stabilizing the face-centered form

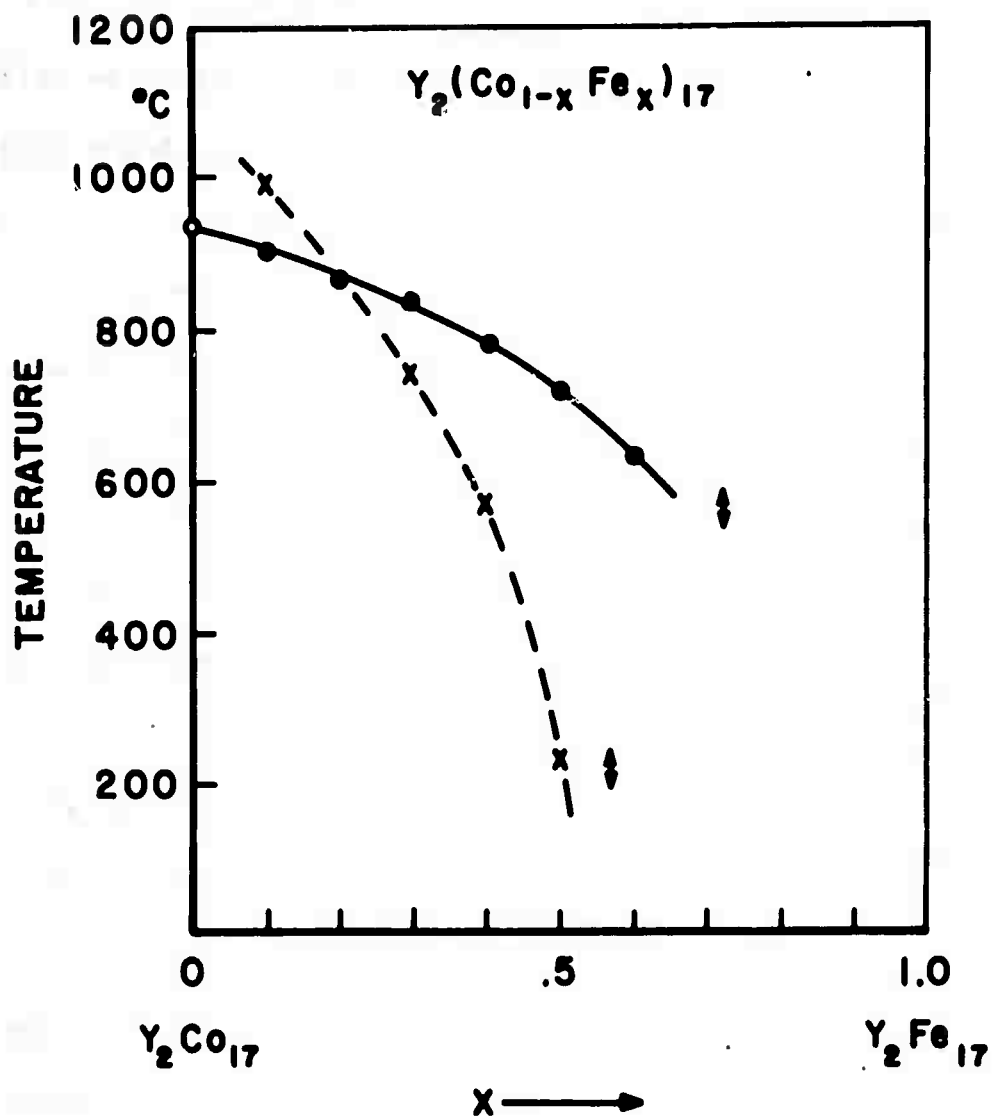


Figure 3.  $T_c$  vs.  $x$  for  $Y_2(Co_{1-x}Fe_x)_{17}$ .

(austenite) down to  $\sim 200^{\circ}\text{C}$  or lower in the iron-rich Co-Fe alloys. We shall pursue these questions further, bringing to bear other tools such as DTA, x-ray diffraction, and electron microprobe analysis.

The TMA spectra obtained on Sm-Co-Fe alloys on both ends of the quasi-binary system are relatively uneventful and simple to interpret. Figure 4 is a summary of the results for this system. Again, the DTA and the TMA data for  $T_c$  agree very closely in the range in which they overlap. Only the point for  $x = 0.5$  deviates from the smooth line of  $T_c$  versus  $x$ , but it is suspected that this is due to a mixup in the alloys and that this sample in fact had  $x = 0.4$ . The analysis will be repeated with a newly-prepared sample. For some of the samarium alloys in the middle of the system, an additional rather pronounced step in the TMA curves was observed between  $900^{\circ}$  and  $1000^{\circ}\text{C}$ , which is  $100^{\circ}$  to  $300^{\circ}$  above the Curie point of the  $\text{Sm}_2(\text{Co}, \text{Fe})_{17}$  phases. This event also exhibited a thermal hysteresis, which was generally small but amounted to  $50^{\circ}$  difference between heating and cooling for  $x = 0.3$ . This behavior is illustrated in Figure 5, using as an example the alloy  $\text{Sm}_2(\text{Co}_{.4}\text{Fe}_{.6})_{17}$ . The physical nature of the transition indicated by this "TMA event" is not clear at this time, and no corresponding events were found in differential thermal analysis. It is likely that some of the speculations made below in connection with the behavior of the cerium alloys apply here, too.

In the system  $\text{Ce}_2(\text{Co}_{1-x}\text{Fe}_x)_{17}$  a much more complex behavior is observed. For alloys in the middle of the quasi-binary system, several

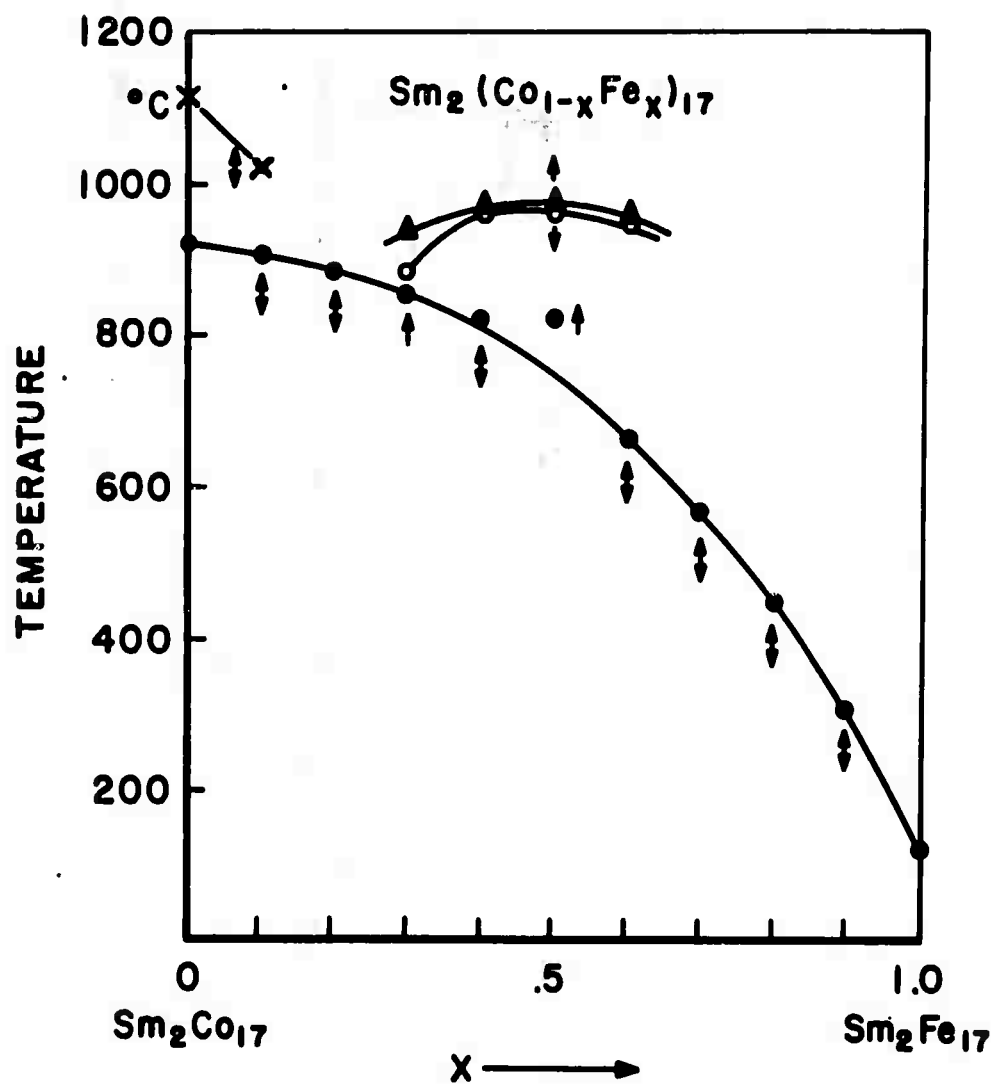


Figure 4.  $T_c$  vs.  $x$  for  $\text{Sm}_2(\text{Co}_{1-x}\text{Fe}_x)_{17}$ .

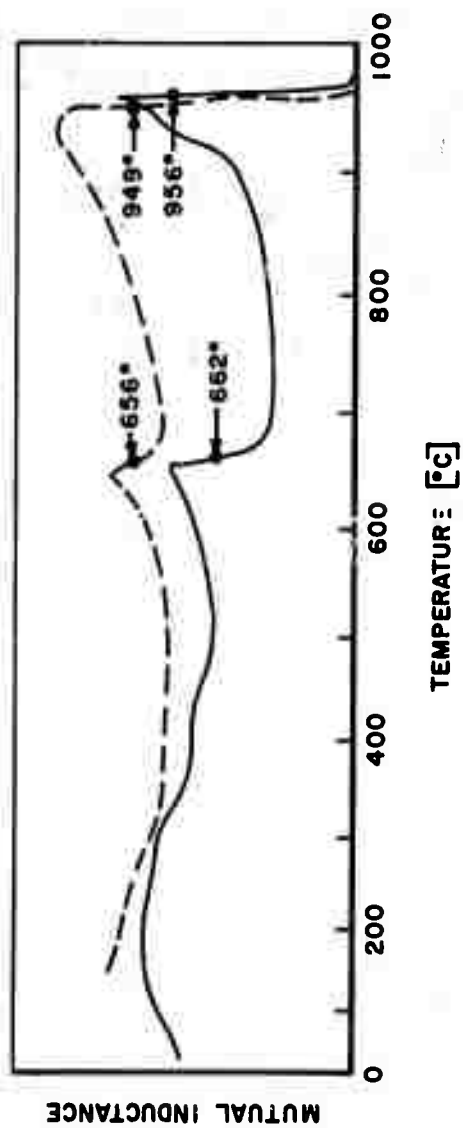


Figure 5. TMA spectrum of  $\text{Sm}_2(\text{Co}_{0.4}\text{Fe}_{0.6})_{17}$  alloy. Solid line is the heating curve; dashed line is the cooling curve.

pronounced steps in the temperature dependence of the initial permeability are seen in the TMA spectra. This is illustrated in Figure 6, a TMA spectrum for  $\text{Ce}_2(\text{Co}_{.4}\text{Fe}_{.6})_{17}$ . We believe the lowest-temperature step to correspond to the Curie point proper of the rhombohedral 2-17 phase. Note that it is observed only on heating, not on cooling. It is followed by a minor wiggle in the curve, and then another pronounced maximum followed by a sharp step down. This upper transition occurs on heating around  $800^\circ$  to  $850^\circ\text{C}$  in several of the alloys, but  $100$ - $200^\circ$  lower on cooling. Figure 7 summarizes the various TMA events found in the alloys of this system. This complex and irreversible behavior is so far unexplained. Some preliminary x-ray work<sup>(11)</sup> appears to support the reasoning that the 2-17 compound becomes unstable upon heating somewhere between  $750^\circ$  and  $850^\circ\text{C}$ , that is dissociates into a  $\text{Ce}(\text{Co}, \text{Fe})_2$  phase and an iron-cobalt solid solution alloy, and that this phase transition is irreversible under the conditions of our TMA cycle. However, it is also possible that an oxidation reaction of the powder used in the TMA plays a major role. Clarification of the matter will require additional experimentation using metallography, x-ray diffraction and magnetic measurements. However, this problem has so far been neglected because its solution seems to be of secondary importance for the attainment of the goal of the contract.

Table I is a listing of all the heating and cooling cycles performed on  $\text{R}_2(\text{Co}, \text{Fe})_{17}$  alloys to date. It gives details of the heat treatment of each

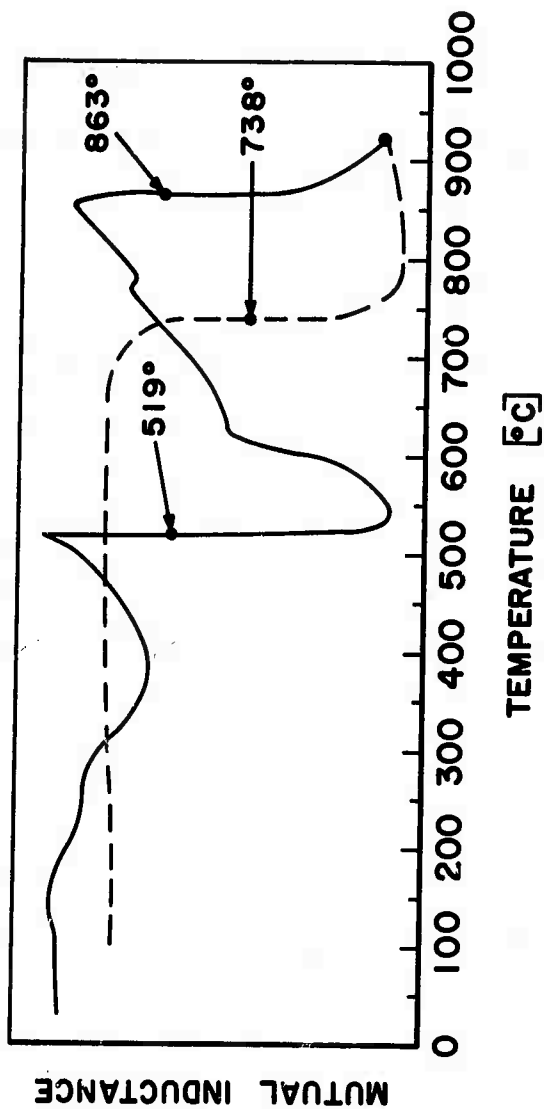


Figure 6. TMA spectrum of  $\text{Ce}_2(\text{Co}_{.4}\text{Fe}_{.6})_{17}$  alloy. Solid line is the heating curve; dashed line is the cooling curve.

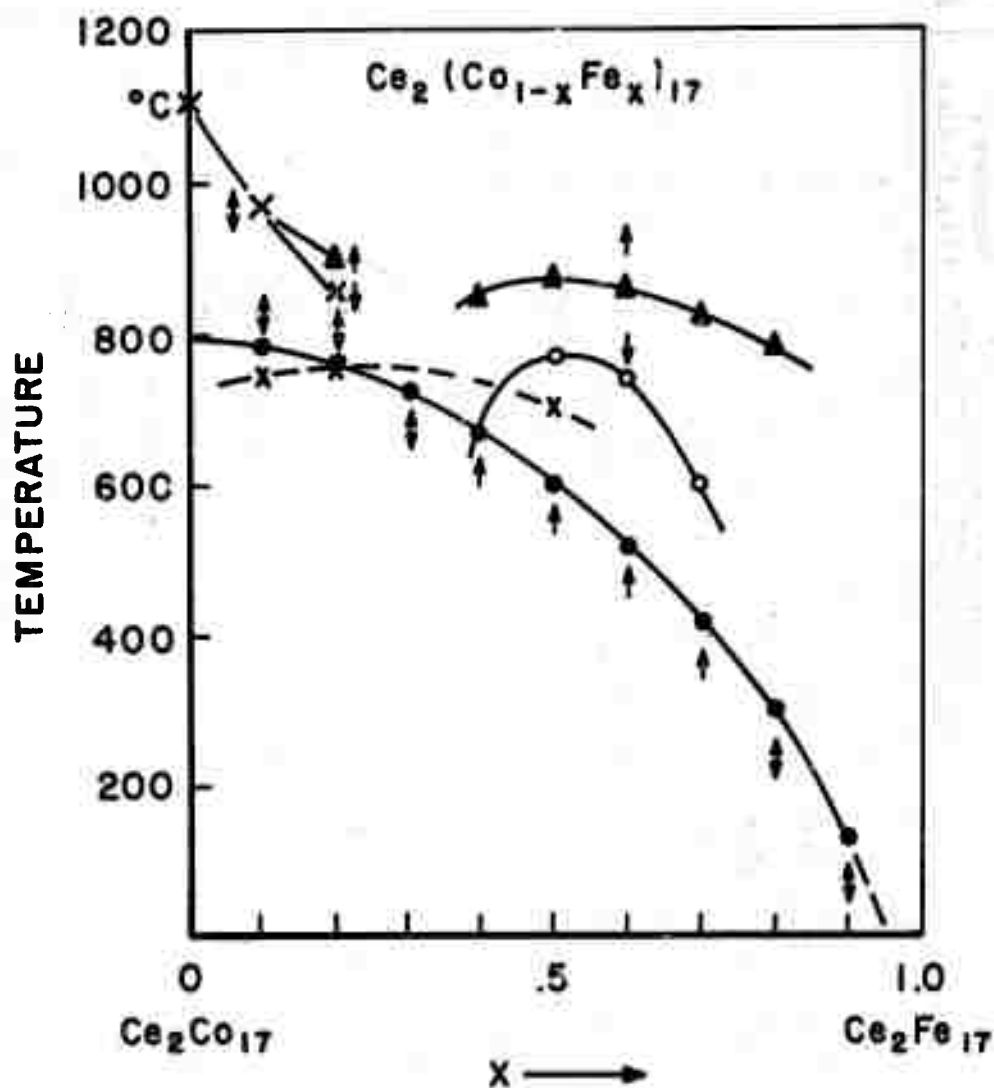


Figure 7.  $T_c$  vs.  $x$  and temperatures of other irregularities in the TMA spectra of  $\text{Ce}_2(\text{Co}_{1-x}\text{Fe}_x)_{17}$  phases.

TABLE I

LIST OF  $R_2(\text{Co}, \text{Fe})_{17}$  ALLOYS THERMOMAGNETICALLY ANALYZED

Alloy Code	Alloy Composition	Heat Treatment		Number of TMA Cycles	Peak Temperature Reached in TMA ( $^{\circ}\text{C}$ )
		Time (hrs)	Temp. ( $^{\circ}\text{C}$ )		
AR-757	$\text{Y}_2(\text{Co}_{.9}\text{Fe}_{.1})_{17}$	6	1050	1	1032
AR-766	$\text{Y}_2(\text{Co}_{.8}\text{Fe}_{.2})_{17}$	6	1050	1	1017
AR-773	$\text{Y}_2(\text{Co}_{.7}\text{Fe}_{.3})_{17}$	7	1050	1	1017
AR-777	$\text{Y}_2(\text{Co}_{.6}\text{Fe}_{.4})_{17}$	6	1200	1	1021
AR-787	$\text{Y}_2(\text{Co}_{.5}\text{Fe}_{.5})_{17}$	6	1200	2	1040
AR-899	$\text{Y}_2(\text{Co}_{.4}\text{Fe}_{.6})_{17}$	70	1150	1	1055
AR-789	$\text{Sm}_2(\text{Co}_{.9}\text{Fe}_{.1})_{17}$	6	1200	3	1121
AR-815	$\text{Sm}_2(\text{Co}_{.8}\text{Fe}_{.2})_{17}$	18	1200	1	1134
AR-816	$\text{Sm}_2(\text{Co}_{.7}\text{Fe}_{.3})_{17}$	18	1200	1	1139
AR-827	$\text{Sm}_2(\text{Co}_{.6}\text{Fe}_{.4})_{17}$	20	1200	1	1010
AR-828	$\text{Sm}_2(\text{Co}_{.5}\text{Fe}_{.5})_{17}$	20	1200	2	1040
AR-883	$\text{Sm}_2(\text{Co}_{.4}\text{Fe}_{.6})_{17}$	90	1100	2	981
AR-882	$\text{Sm}_2(\text{Co}_{.3}\text{Fe}_{.7})_{17}$	90	1100	1	658
AR-847	$\text{Sm}_2(\text{Co}_{.2}\text{Fe}_{.8})_{17}$	30	1150	1	625
AR-848	$\text{Sm}_2(\text{Co}_{.1}\text{Fe}_{.9})_{17}$	30	1150	1	400
AR-755	$\text{Ce}_2(\text{Co}_{.9}\text{Fe}_{.1})_{17}$	6	1050	3	1023
AR-833	$\text{Ce}_2(\text{Co}_{.9}\text{Fe}_{.1})_{17}$	18	1100	1	1014
AR-764	$\text{Ce}_2(\text{Co}_{.8}\text{Fe}_{.2})_{17}$	6	1050	2	1023

TABLE I (concluded)  
LIST OF  $R_2(\text{Co}, \text{Fe})_{17}$  ALLOYS THERMOMAGNETICALLY ANALYZED

Alloy Code	Alloy Composition	Heat Treatment		Number of TMA Cycles	Peak Temperature Reached in TMA ( $^{\circ}\text{C}$ )
		Time (hrs)	Temp. ( $^{\circ}\text{C}$ )		
AR-834	$\text{Ce}_2(\text{Co}_{.8}\text{Fe}_{.2})_{17}$	18	1000	1	998
AR-771	$\text{Ce}_2(\text{Co}_{.7}\text{Fe}_{.3})_{17}$	7	1050	1	866
AR-835	$\text{Ce}_2(\text{Co}_{.7}\text{Fe}_{.3})_{17}$	18	1100	1	1021
AR-775	$\text{Ce}_2(\text{Co}_{.6}\text{Fe}_{.4})_{17}$	6	1050	3	911
AR-785	$\text{Ce}_2(\text{Co}_{.5}\text{Fe}_{.5})_{17}$	7	1050	4	916
AR-840	$\text{Ce}_2(\text{Co}_{.4}\text{Fe}_{.6})_{17}$	18	1000	4	921
AR-841	$\text{Ce}_2(\text{Co}_{.3}\text{Fe}_{.7})_{17}$	18	1000	2	931
AR-842	$\text{Ce}_2(\text{Co}_{.2}\text{Fe}_{.8})_{17}$	18	1000	2	915
AR-843	$\text{Ce}_2(\text{Co}_{.1}\text{Fe}_{.9})_{17}$	18	1000	2	908

alloy before the start of the thermomagnetic analysis and the highest temperature to which the TMA was carried. It identifies the alloys by the numbers assigned when they were prepared.

#### D. MAGNETIZATION MEASUREMENTS

(Mildrum, Walsh, Strnat) .

Magnetization measurements were made with the oscillating specimen magnetometer on loose powder samples of  $R_2(Co_{1-x}Fe_x)_{17}$  phases to determine the room-temperature saturation. Many samples in five quasi-binary systems were measured. Tentative results are shown in Table II. The comparison ranges include those for which easy-axis behavior was found.

TABLE II  
TENTATIVE RESULTS OF SATURATION MAGNETIZATION  
MEASUREMENTS ON  $R_2(Co_{1-x}Fe_x)_{17}$  PHASES

R	x(Fe Fraction)	$\sigma$ (emu/g)*
Sm	0 - 0.5	109 - 143
Pr	0 - 0.5	128 - 159
Ce	0 - 0.4	103 - 130
Y	0 - 0.5	125 - 150
MM	0.1 - 0.5	118 - 145

\*Values of  $\sigma$  correspond to the listed extremes of x.

For the quantitative study of crystal anisotropy, magnetically oriented, epoxy-bonded powder samples were made of the same alloys. Easy-axis and hard-axis magnetization curves were measured on these in

fields up to 20 kOe. Figure 8 shows three sets of such magnetization curves measured on three different alloys in the  $\text{Sm}_2(\text{Co}_{1-x}\text{Fe}_x)_{17}$  alloy system, namely, the terminal compound  $\text{Sm}_2\text{Co}_{17}$  and the alloys for  $x = 0.4$  and  $0.5$  which are near the end of the easy-axis region. The curves were measured up to 20 kOe and extrapolated beyond this point. While it was found that smaller iron additions of  $x = 0.1$  and  $0.2$  increased the anisotropy field slightly above the value of  $H_A \approx 60\text{-}70$  kOe of  $\text{Sm}_2\text{Co}_{17}$ , iron additions as high as  $x = 0.4$  and  $0.5$  bring a reduction of the crystal anisotropy. However, the anisotropy field values are very substantial up to  $x = 0.5$ . This indicates that there is a realistic chance that excellent permanent magnets may be produced on the basis of  $\text{Sm}_2(\text{Co}_{1-x}\text{Fe}_x)_{17}$  phases.

Figure 9 shows similar sets of easy-axis and hard-axis magnetization curves for three Pr-Co-Fe alloys. Here, the anisotropy field is highest in the range  $x = 0.3$  to  $0.5$ . The highest values of the anisotropy field in this system are only between 20 and 30 kOe, that is, less than half of those found in the samarium system.

Figure 10 shows magnetization curves for aligned powders of three mischmetal-cobalt-iron alloys. Here, the maximum of the anisotropy occurs for  $x = 0.3$ , and even this highest anisotropy field is only on the order of 10 kOe, substantially smaller than the anisotropy fields for the praseodymium or samarium systems.

For the  $\text{R}_2(\text{Co,Fe})_{17}$  phases, as for the  $\text{RCo}_5$  phases, it appears that samarium has a certain "magic" quality of being able to induce very high crystal anisotropy. The anisotropy fields measured on these 2-17 phases

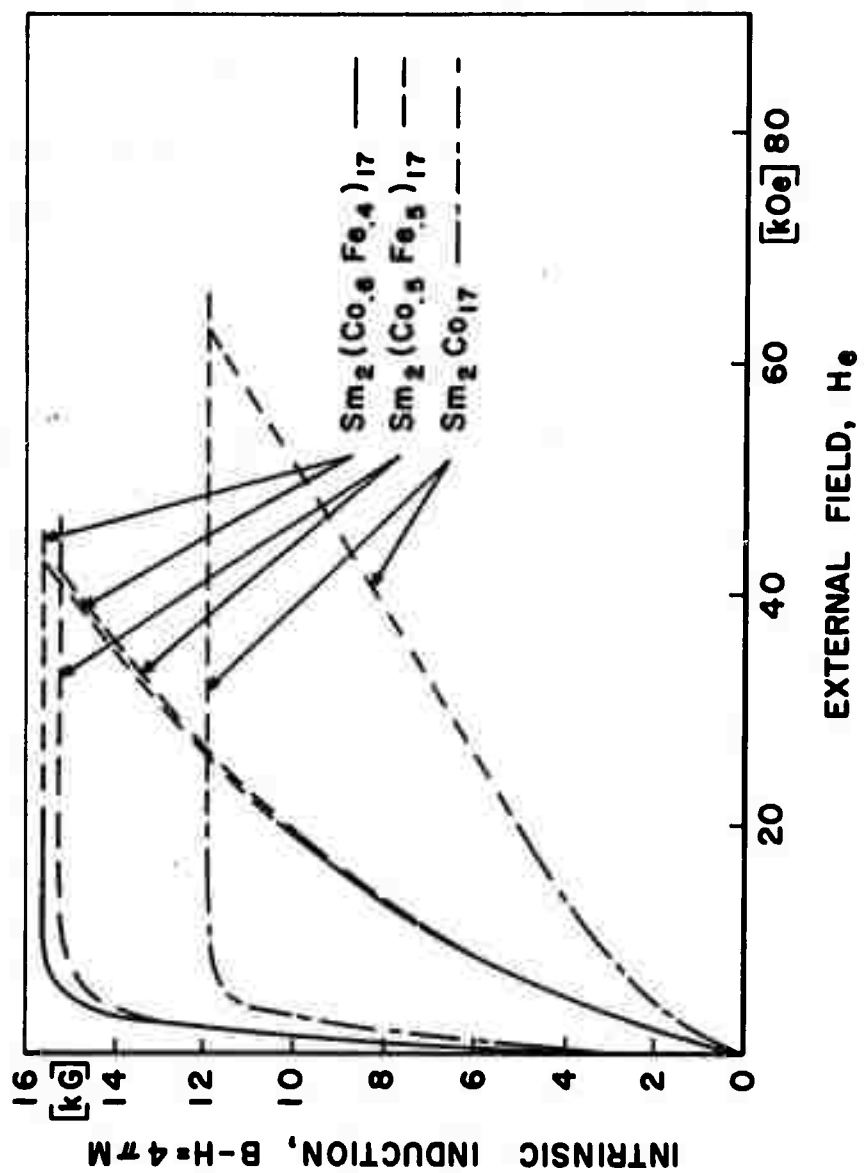


Figure 8. Easy-axis and hard-axis magnetization curves measured on oriented powders of three  $\text{Sm}_2(\text{Co}_{1-x}\text{Fe}_x)_{17}$  alloys.

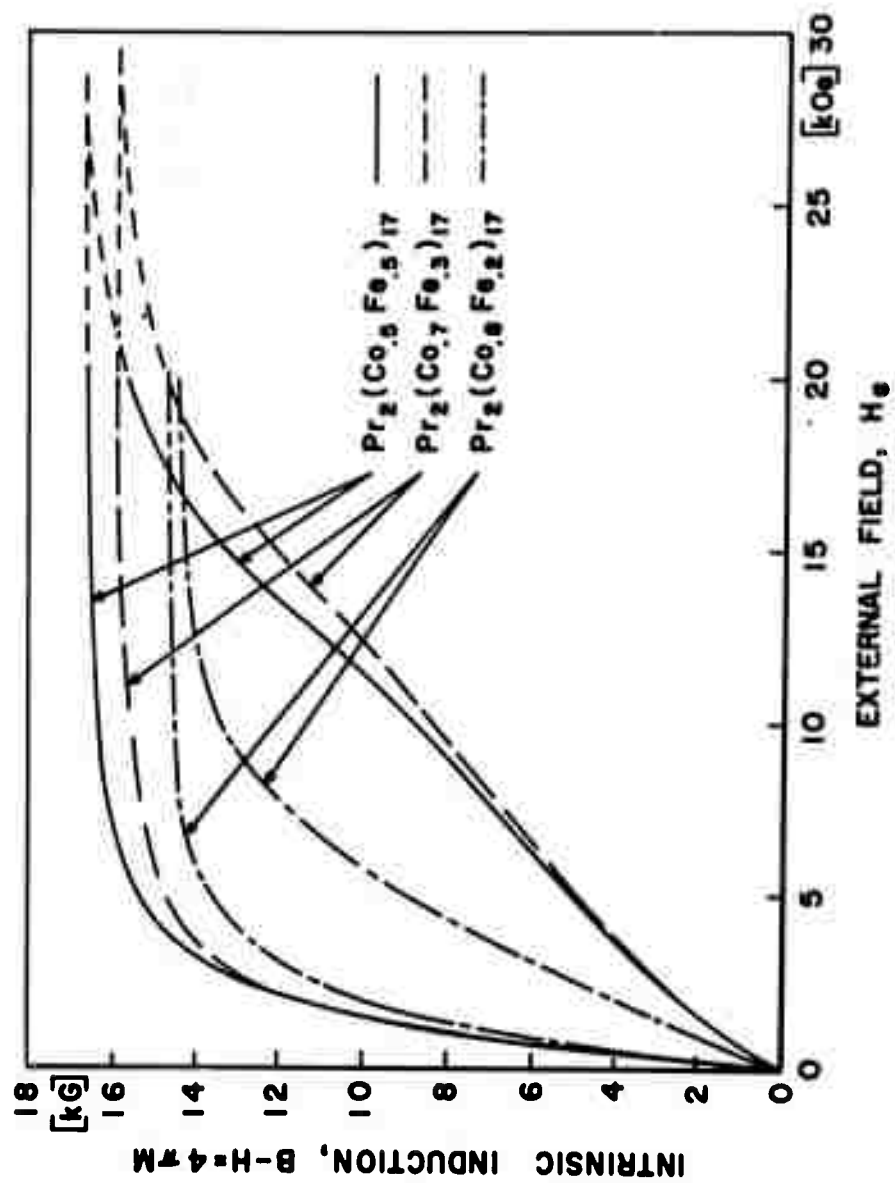


Figure 9. Magnetization curves measured on oriented powders of three  $Pr_2(Co_{1-x}Fe_x)_{17}$  alloys.

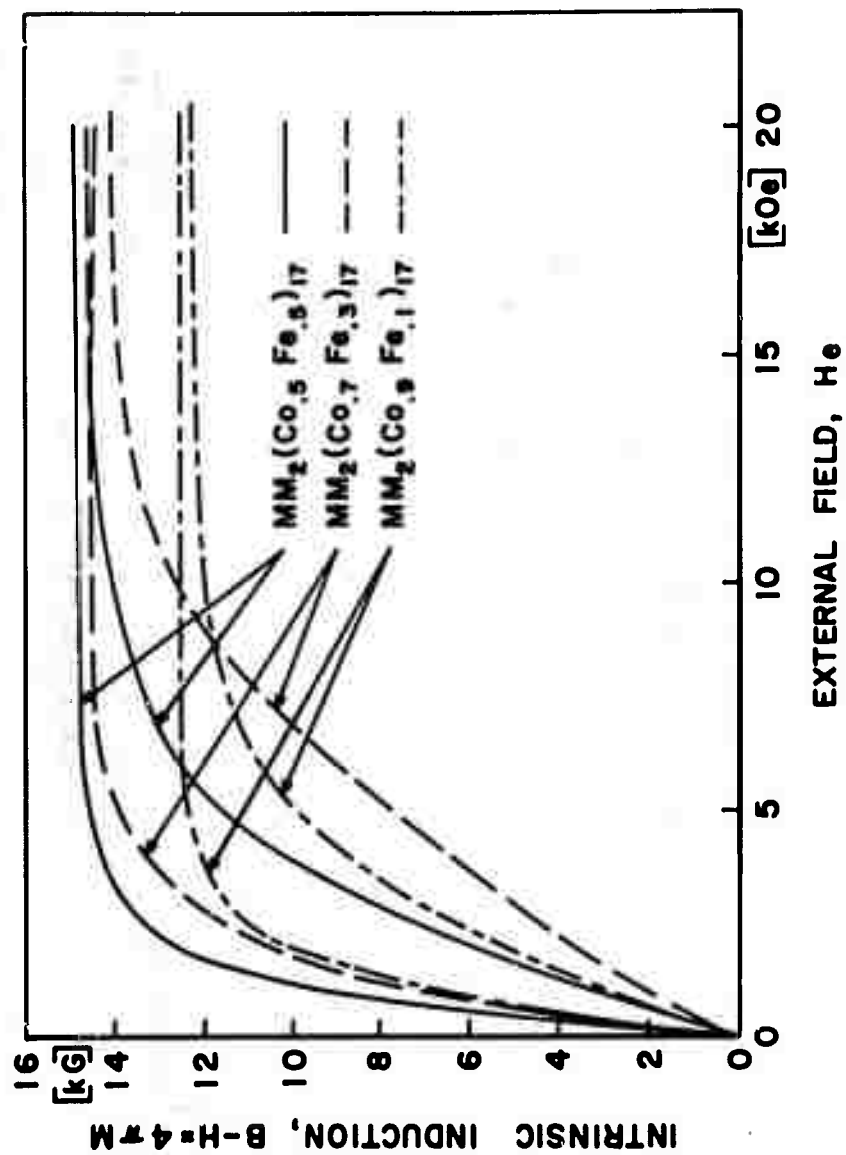


Figure 10. Magnetization curves measured on oriented powders of three  $\text{MM}_2(\text{Co}_{1-x}\text{Fe}_x)_{17}$  alloys.

are substantially lower than those of the  $\text{RCo}_5$  compounds. However, if we compare them with the value of the anisotropy field of barium ferrite, for which  $H_A = 17 \text{ kOe}$ , they appear nevertheless quite respectably high. Considering that barium ferrite has become a highly successful commercial permanent magnet, we must indeed give the  $\text{R}_2(\text{Co,Fe})_{17}$  compounds serious consideration, and especially, we must consider the Sm-Co-Fe alloys as very promising candidates for second-generation rare earth permanent magnets.

Early attempts to produce high coercivity in fine powders of  $\text{Sm}_2\text{Co}_{17}$  by grinding did not have encouraging results. The highest  $M H_c$  values achieved were only between 1000 and 2000 Oe. But it seems that by properly applying the present knowledge about the liquid-phase sintering of  $\text{RCo}_5$  compound magnets, it should be possible to bring about intrinsic coercive forces which are a substantial fraction of the anisotropy field and thus high enough to exploit the high energy-product potential of the 2-17 phases.

#### E. THE PROSPECTS FOR $\text{R}_2(\text{Co,Fe})_{17}$ MAGNETS

We have conducted some preliminary experiments trying to sinter ball milled  $\text{Sm}_2\text{Co}_{17}$  powders to which the commonly used 60% Sm/40% Co alloy was added as the sintering aid. In these experiments we have used as the guiding hypothesis the concept that, during sintering, epitaxial shells of a compound richer in the rare earth can form around the core of the base metal alloy, and that effective domain wall pinning can take place in these epitaxial layers.<sup>(12)</sup> While the concept was first invented to explain some

observations during the sintering of  $\text{PrCo}_5$  with a praseodymium-rich sintering aid, it can certainly be applied also to the system in which  $\text{Sm}_2\text{Co}_{17}$  is the base metal. If a samarium-rich sintering aid is used, the first epitaxial shell to form would be  $\text{SmCo}_5$ . Since  $\text{SmCo}_5$  has the highest anisotropy known, any imperfections in this shell should be very effective pinning sites. We were most encouraged to find intrinsic coercive forces up to  $M H_c = 9600$  Oe in these initial, and very unsystematic, experiments. We take these results as strong encouragement that, eventually, it should indeed be possible to produce permanent magnets from 2-17 alloys which will have energy products in excess of those of the  $\text{RCO}_5$  magnets.

While it is very desirable for many applications to have intrinsic coercive forces ( $M H_c$ , in Oe) in excess of the value of the residual magnetization ( $B_r$ , in G), energy products near the theoretical limit of  $(B_s/2)^2$  can in principle be achieved with coercive forces which are only slightly in excess of  $B_s/2$ . For the example of  $\text{Sm}_2\text{Co}_{17}$ , which has a saturation of  $4\pi B_s = 12$  kG, a coercivity  $M H_c > 6$  kOe should be sufficient to permit energy products approaching 36 MGOe, provided all other factors can be optimized.

In view of the favorable experimental results reported above, we are encouraged to indulge in some speculations about the energy products one may hope to achieve with magnets based on the 2-17 phases. Let us first consider Figure 11 which shows the room temperature saturation values for all binary  $\text{R}_2\text{Co}_{17}$  and  $\text{R}_2\text{Fe}_{17}$  compounds and, for comparison, those of the  $\text{RCO}_5$ . We can see that the maximum values which occur for

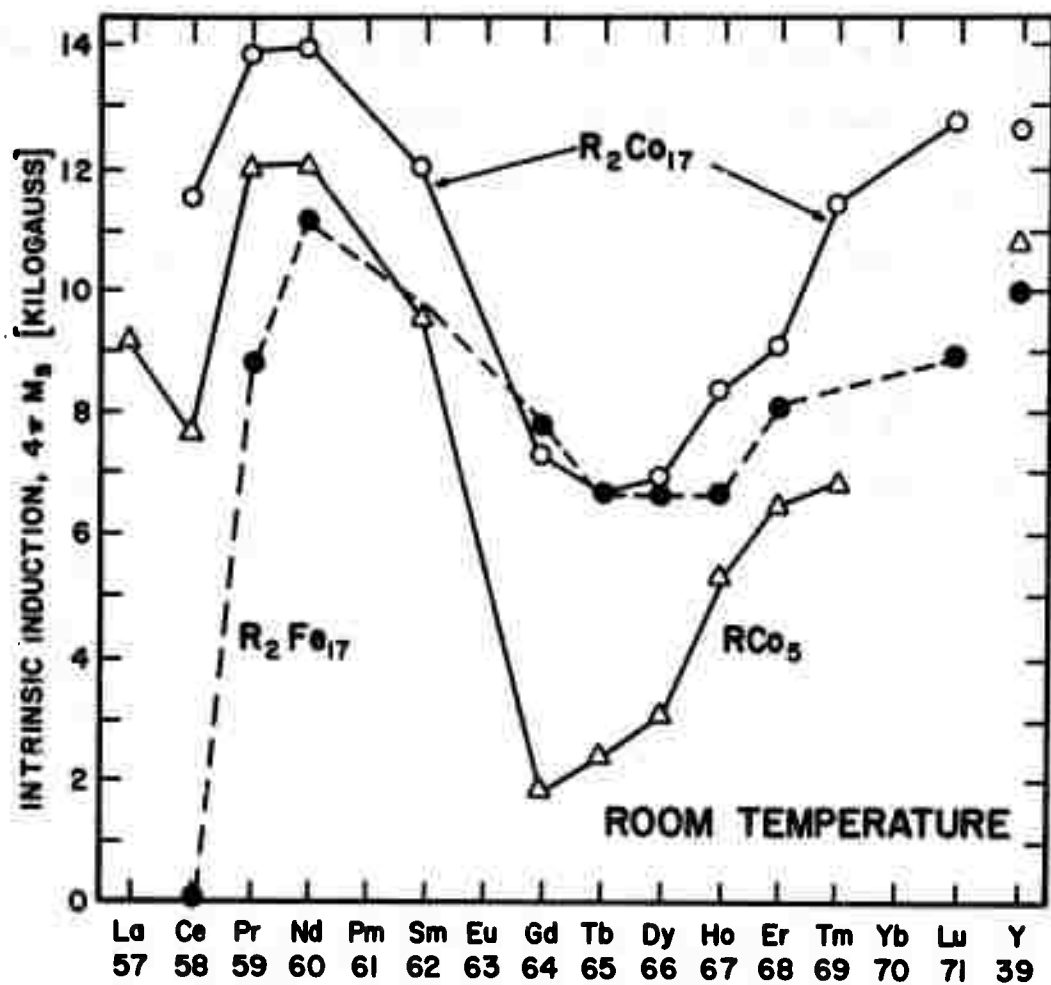


Figure 11. Saturation induction values at room temperature for the compounds  $R_2Co_{17}$ ,  $R_2Fe_{17}$ , and  $RCo_5$ .

$R = \text{Pr}$  and  $\text{Nd}$ , are  $B_g = 14$  kG. Even the lowest values of any  $R_2\text{Co}_{17}$  compounds, those for  $R = \text{Gd}$ ,  $\text{Tb}$  and  $\text{Dy}$ , are still near 7 kG. Let us remember that this high saturation is combined with high Curie temperatures near  $900^\circ\text{C}$ , a very desirable situation indeed. The saturation values for the  $R_2\text{Fe}_{17}$  phases would also be attractively high (Fig. 11), but their Curie temperatures are quite low, namely  $T_c < 180^\circ\text{C}$ .

We have seen that mixed phases of the composition of  $R_2(\text{Co}_{1-x}\text{Fe}_x)_{17}$  exist for all light rare earths and for all values of  $x$ . We have also seen that in the systems in which  $R = \text{Y}$ ,  $\text{Ce}$ ,  $\text{Pr}$ ,  $\text{Sm}$ , and  $\text{MM}$ , the introduction of some iron in the lattice induces easy-axis anisotropy and thus creates favorable conditions for hard magnetic behavior. Let us also remember that we found earlier during the work under this contract that the introduction of iron in these phases in quantities up to  $x \approx 0.5$  does not significantly depress  $T_c$ . The Curie points remain above  $600^\circ\text{C}$  up to this composition in all the alloy systems of interest.

The theoretical limits for the energy product of these mixed phases are even higher than for the corresponding binary  $R_2\text{Co}_{17}$  compounds. It is well known that  $\text{Co}_{1-x}\text{Fe}_x$  alloys with  $x \approx 0.5$  have the highest room-temperature saturation values of any known substance, higher than those of either iron or cobalt (See Fig. 12). The same behavior carries over into the mixed quasi-binary phases  $R_2(\text{Co}_{1-x}\text{Fe}_x)_{17}$  as is also illustrated in Figure 12 for the example  $\text{Y}_2(\text{Co}_{1-x}\text{Fe}_x)_{17}$ . The higher saturation values in the middle of the quasi-binary system correspond to higher potential energy products.

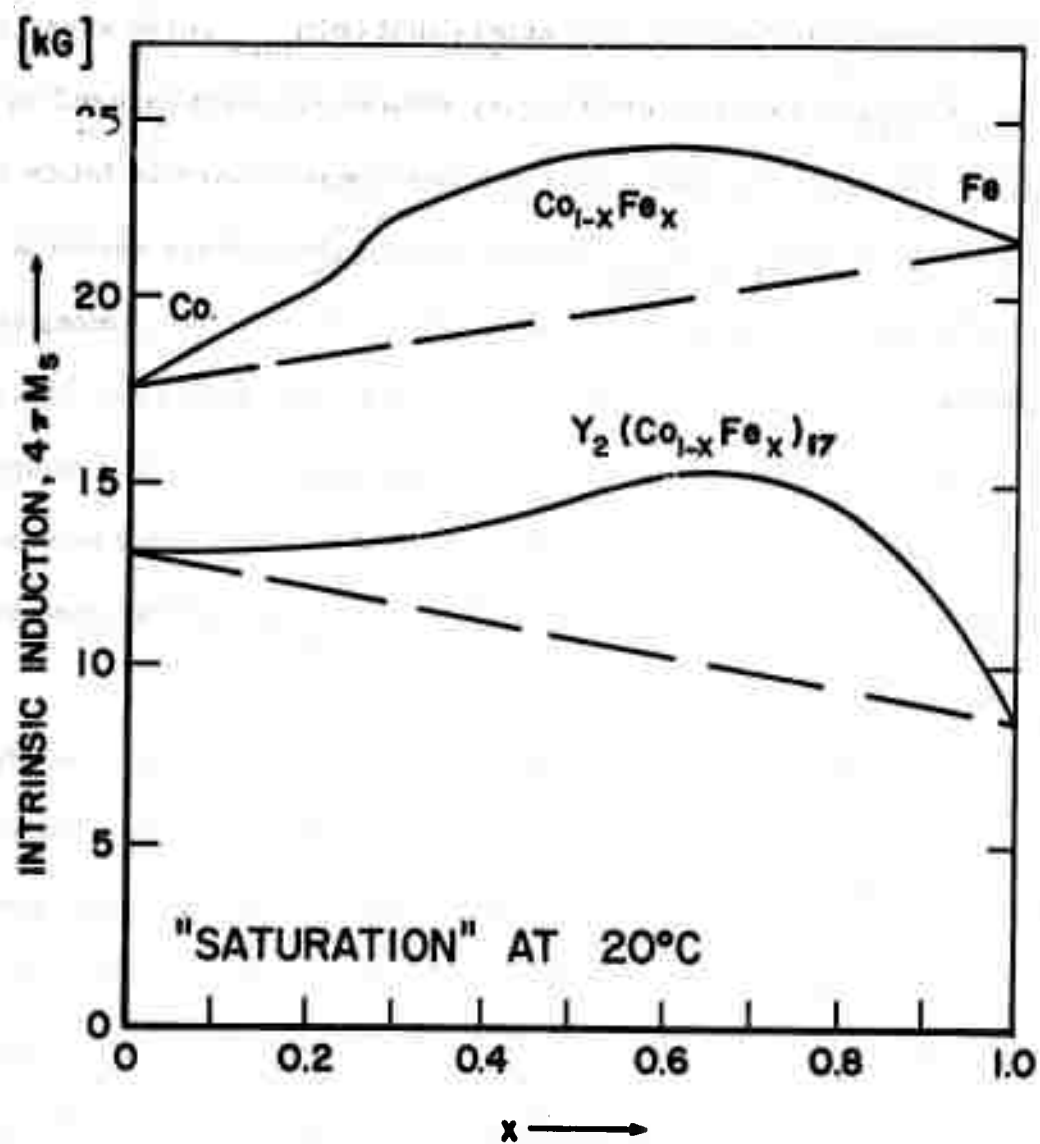


Figure 12. Composition dependence of the room-temperature saturation in the systems Co-Fe and  $Y_2Co_{17} - Y_2Fe_{17}$ .

Finally, in Figure 13, we show how the potential static energy products of several of the 2-17 phases compare with the highest energy products available in present commercial magnet types and the best laboratory samples of  $\text{SmCo}_5$ . The upper-limit  $(BH)_{\text{max}}$  curve shown for  $\text{Sm}_2(\text{Co}_{1-x}\text{Fe}_x)_{17}$  is based on preliminary saturation data measured on aligned powder samples. This curve reaches a peak of over 60 MGOe for  $x = 0.4$ . In the  $\text{Pr}_2(\text{Co}_{1-x}\text{Fe}_x)_{17}$  system, even higher values should be possible, but reliable magnetization data are as yet lacking. Among the 2-17 phases even those of the heavier rare earths promise rather high energy products. This is illustrated by the easy-axis type binary cobalt compounds  $\text{Er}_2\text{Co}_{17}$  and  $\text{Tm}_2\text{Co}_{17}$ . Consequently, in contrast to the situation with  $\text{RCo}_5$ , one could at least tolerate substantial quantities of heavy rare earths in  $\text{R}_2(\text{Co,Fe})_{17}$  magnet alloys.

It will indeed be a challenging task for the coming years to attempt the practical realization of these hopes and to develop even better rare earth-transition metal magnets than those available at the present time. The next step toward this practical objective must be by systematic sintering studies aimed at creating coercive forces of  $M H_c > B_s / 2$  without sacrificing too much of the saturation. The statements made above suggest also that the present investigation of the magnetic properties of ternary R-Co-Fe alloys of the 2-17 type should be expanded to include some phases of the heavy rare earth metals.

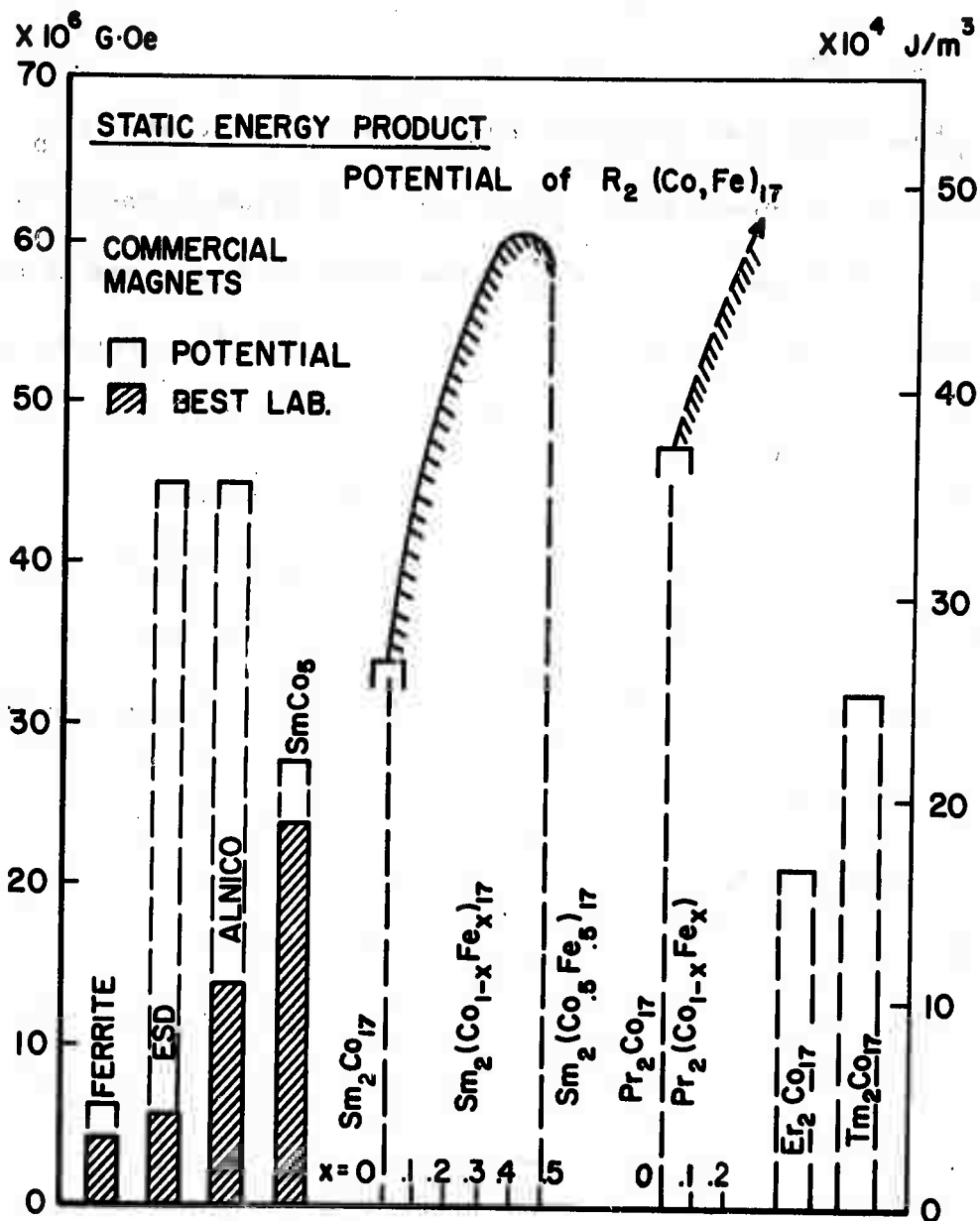


Figure 13. Theoretically possible energy products for magnets made from selected  $R_2(Co,Fe)_{17}$  phases compared to best experimental and theoretical values for other magnet types.

SECTION II  
METALLURGICAL AND MAGNETIC PROPERTIES  
OF SOME  $\text{Nd}_{1-x}\text{R}_x\text{Co}_5$  ALLOYS

A. INTRODUCTION

$\text{NdCo}_5$  has the highest saturation magnetization of all of the  $\text{RCo}_5$  phases, and a high Curie temperature. Moreover, neodymium is one of the most abundant of the rare earth metals.  $\text{NdCo}_5$  displays an easy c-axis and high magnetocrystalline anisotropy, but only when heated appreciably above room temperature.

We are studying the effect of alloying additions of the type  $\text{Nd}_{1-x}\text{R}_x\text{Co}_5$  (when R is any of several of the other rare earth metals) on the transition point of  $\text{NdCo}_5$  from easy basal plane to easy c-axis anisotropy. We are also studying the effect of these alloying additions on other pertinent magnetic and metallurgical properties.

B. ALLOY PREPARATION (Leasure, Ray)

The alloys were prepared by arc melting the elemental constituents. Many of these were given subsequent homogenization heat treatments. The same arc melting and homogenization procedures used for  $\text{R}_2\text{Co}_{17}$  alloys were employed. These have been described in a previous report<sup>(13)</sup>. In each case, the weights of the rare earth elements required to produce nominally stoichiometric  $\text{Nd}_{1-x}\text{R}_x\text{Co}_5$  alloys were increased by 2.0 wt. % to compensate for the oxygen present in the elemental constituents. Initial sets of alloys were prepared with R = Ce, Pr, and Y and x-values of 0.25, 0.5 and 0.75 for each set.

### C. THERMAL ANALYSIS (Biermann, Ray)

Differential thermal analyses (DTA) were performed on at least one member of each set. The observed melting or peritectic temperatures and Curie points are tabulated in Table III. The melting or peritectic temperatures of the ternary alloys appear to be linear functions of composition, as illustrated in Figure 14. These melting curves were used to determine the maximum annealing temperatures to optimize grain growth conditions for preparing large crystals of the mixed phases.

In contrast to the melting and peritectic temperatures, the Curie temperatures observed by DTA for the  $\text{Nd}_{1-x}\text{R}_x\text{Co}_5$  phases do not appear to be monotonic functions of composition. Whether this is actually the case will be checked by the more sensitive TMA measurements.

### D. LATTICE CONSTANTS (Geis, Harmer, Ray)

Lattice constants were determined from powder x-ray diffraction patterns obtained with a General Electric XRD-6 diffractometer and Type 700 detector system. The diffraction patterns were obtained with V-filtered  $\text{Cr K}_\alpha$  radiation. Lattice constant data were refined by the Vogel and Kempter method<sup>(14)</sup> with the aid of the RCA Spectra 70/40 computer.

Lattice constants for  $\text{Nd}_{1-x}\text{R}_x\text{Co}_5$  phases with  $\text{R} = \text{Ce}$  and  $\text{Pr}$  and  $x = 0, 0.25, 0.5, 0.75,$  and  $1.0$  are given in Table IV. The lattice constants of the mixed  $\text{Nd}_{1-x}\text{R}_x\text{Co}_5$  phases do not appear to vary smoothly with composition. This may be because the single phase fields for these alloys are relatively wide and the alloy-to-alloy variations in the total rare earth to

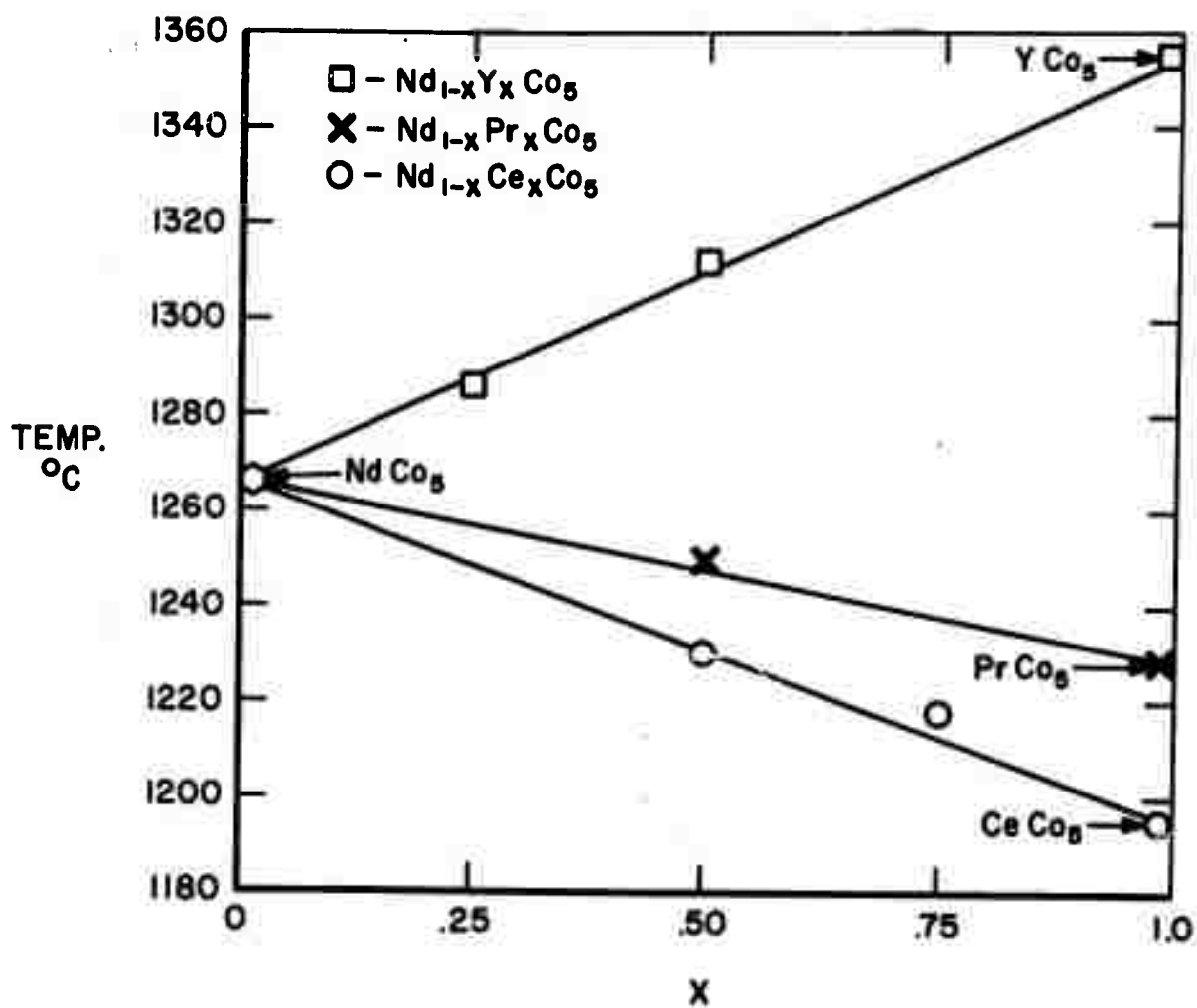


Figure 14. Melting and peritectic temperatures for  $\text{Nd}_{1-x}\text{R}_x\text{Co}_5$  alloys.

TABLE III  
THERMAL EVENTS OBSERVED BY DTA FOR  
SOME BINARY AND TERNARY  $\text{RCO}_5$  ALLOYS

Alloy No.	Nominal Composition	Thermal History	Curie Temperature ( $^{\circ}\text{C}$ )	Peritectic or Melting Temp. ( $^{\circ}\text{C}$ )
AR-971	$\text{YCo}_5$	168 hrs at $1225^{\circ}\text{C}$	657	1353
AR-969	$\text{Nd}_{0.5}\text{Y}_{0.5}\text{Co}_5$	as cast	645	1312
AR-968	$\text{Nd}_{0.75}\text{Y}_{0.25}\text{Co}_5$	as cast	649	1286
AR-874	$\text{PrCo}_5$	90 hrs at $1100^{\circ}\text{C}$	625	1229
AR-974	$\text{Nd}_{0.5}\text{Pr}_{0.5}\text{Co}_5$	as cast	620 very weak	1250
AR-995	$\text{CeCo}_5$	168 hrs at $1100^{\circ}\text{C}$	not observed	1195
AR-996	$\text{Nd}_{0.25}\text{Ce}_{0.75}\text{Co}_5$	168 hrs at $1100^{\circ}\text{C}$	not observed	1218
AR-978	$\text{Nd}_{0.5}\text{Ce}_{0.5}\text{Co}_5$	as cast	not observed	1230
AR-819	$\text{NdCo}_5$	20 hrs at $1050^{\circ}\text{C}$	643	1266

TABLE IV  
LATTICE CONSTANTS FOR  $\text{Nd}_{1-x}\text{Ce}_x\text{Co}_5$  AND  $\text{Nd}_{1-x}\text{Pr}_x\text{Co}_5$  PHASES

Alloy No.	Nominal Composition	$a_o, \text{\AA}$	$c_o, \text{\AA}$	Heat Treatment
AR- 967	$\text{NdCo}_5$	$5.002 \pm .001$	$3.995 \pm .001$	168 hrs at $1225^\circ\text{C}$
AR- 979	$\text{Nd}_{0.75}\text{Ce}_{0.25}\text{Co}_5$	$4.996 \pm .001$	$3.996 \pm .001$	168 hrs at $1170^\circ\text{C}$
AR- 978	$\text{Nd}_{0.5}\text{Ce}_{0.5}\text{Co}_5$	$4.961 \pm .001$	$4.018 \pm .001$	168 hrs at $1170^\circ\text{C}$
AR- 977	$\text{Nd}_{0.25}\text{Ce}_{0.75}\text{Co}_5$	$4.919 \pm .001$	$4.048 \pm .001$	168 hrs at $1170^\circ\text{C}$
AR-1000	$\text{CeCo}_5$	$4.925 \pm .001$	$4.029 \pm .001$	48 hrs at $1125^\circ\text{C}$
AR- 975	$\text{Nd}_{0.75}\text{Pr}_{0.25}\text{Co}_5$	$4.995 \pm .001$	$4.008 \pm .001$	168 hrs at $1225^\circ\text{C}$
AR- 974	$\text{Nd}_{0.5}\text{Pr}_{0.5}\text{Co}_5$	$5.026 \pm .001$	$3.985 \pm .001$	168 hrs at $1170^\circ\text{C}$
AR- 973	$\text{Nd}_{0.25}\text{Pr}_{0.75}\text{Co}_5$	$5.022 \pm .001$	$3.998 \pm .001$	168 hrs at $1170^\circ\text{C}$
AR- 972	$\text{PrCo}_5$	$5.017 \pm .001$	$3.999 \pm .001$	168 hrs at $1170^\circ\text{C}$

cobalt ratios ( $\text{Nd} + \text{R} / \text{Co}$ ) are as significant as the variations in the intra-rare earth ratios ( $\text{Nd} / \text{R}$ ). The irregular variation of the Curie temperatures discussed previously may also be due to differences in rare earth to cobalt ratios.

#### E. PREPARATION OF SINGLE CRYSTALS

(Shanley, Leasure, Kraus, Ray)

Irregularly shaped single crystals of  $\text{NdCo}_5$ ,  $\text{CeCo}_5$ ,  $\text{PrCo}_5$ , and several mixed  $\text{Nd}_{1-x}\text{Ce}_x\text{Co}_5$  and  $\text{Nd}_{1-x}\text{Pr}_x\text{Co}_5$  phases measuring from 1.5 to 3.0 mm in diameter have been obtained by long-term annealing of the arc melted alloys. The slightly rare earth-rich alloys were wrapped in tantalum foil and annealed in vacuum for one week (168 hours) at temperatures  $50^\circ\text{C}$  to  $100^\circ\text{C}$  below the peritectic melting temperatures of the  $\text{RCo}_5$  phases as determined by DTA. The critical annealing range for rapid grain growth appears to lie between the  $\text{RCo}_5$  and  $\text{R}_2\text{Co}_7$  (or  $\text{R}_5\text{Co}_{19}$ ) peritectic decomposition temperatures for the individual alloys. If the alloy is slightly rare earth-rich, then, in this critical temperature range, the small amount of liquid that will be present in the alloy will speed up the diffusion processes markedly. Typical results of the annealing treatment are illustrated in micrographs of a  $\text{Nd}_{0.5}\text{Ce}_{0.5}\text{Co}_5$  alloy (AR-978). Figure 15 shows the alloy in the as-cast condition under bright field illumination. This alloy is slightly rare earth-rich. The gray phase is the  $\text{RCo}_5$  phase and the lighter phase is either an  $\text{R}_5\text{Co}_{19}$  or an  $\text{R}_2\text{Co}_7$  phase. The gradation of the gray color of the  $\text{RCo}_5$  phase from dark at the centers to light at grain boundaries

suggests "coring" has occurred. The initial portion of the  $\text{RCo}_5$  phase to solidify has a slightly different composition than the last. Figure 16 shows the alloy after a homogenization heat treatment of 168 hours at  $1170^\circ\text{C}$ . Extensive grain growth has taken place. In this case, the micrograph was taken under polarized light to reveal the magnetic domain patterns in the individual grains or crystals.

The annealed alloys were friable to the extent that the alloys could be broken up either by hand or with a needle used as a pick to fragment off small sections. Single crystals were obtained by selecting the most promising appearing fragments as evidenced by their cleavage fractures. Laue x-ray diffraction patterns were taken to confirm that the selected fragments were indeed single crystals and to orient the crystals for magnetic measurements. Figure 17 is a Laue photograph of a  $\text{PrCo}_5$  crystal oriented with its c-axis parallel to the x-ray beam. The diffraction spots correspond closely with the size and shape of the crystal.

#### F. MAGNETIC CURIE TEMPERATURE MEASUREMENTS

(Hartings, Mildrum, Strnat)

The composition dependence of the Curie temperature for the systems  $\text{Nd}_{1-x}\text{Ce}_x\text{Co}_5$  and  $\text{Nd}_{1-x}\text{Pr}_x\text{Co}_5$  was determined using a. c. thermomagnetic analysis (TMA). As usual, we took as the Curie point the temperature of the point of inflection of the steep drop in the curve which follows the Hopkinson maximum on the high-temperature side. Heating and cooling cycles

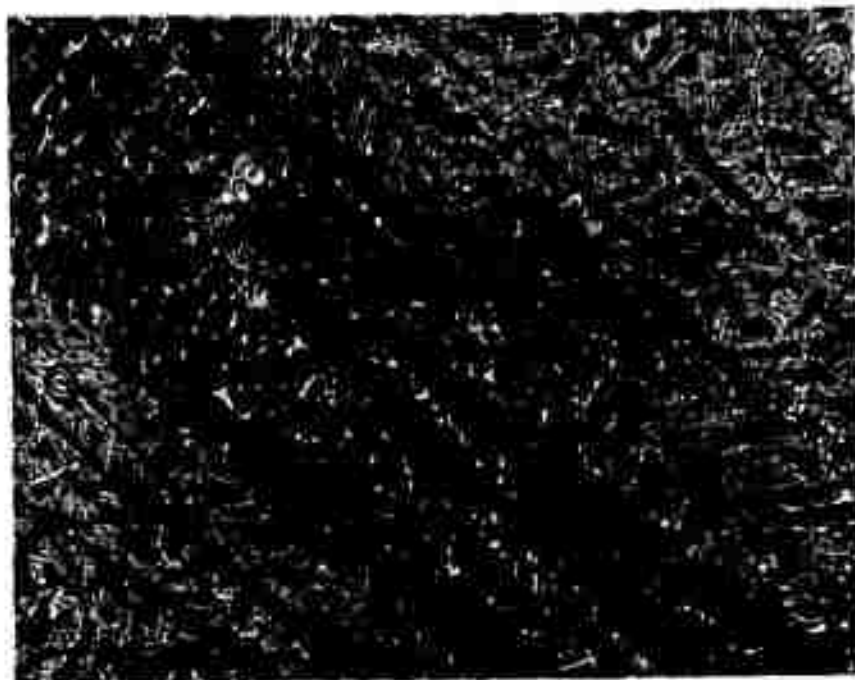


Figure 15. Slightly rare earth rich Nd<sub>0.5</sub>Ce<sub>0.5</sub>Co<sub>5</sub> alloy (AR-978) as-cast. The gray phase is either an R<sub>5</sub>Co<sub>19</sub> or R<sub>2</sub>Co<sub>7</sub> phase. Bright field illumination.

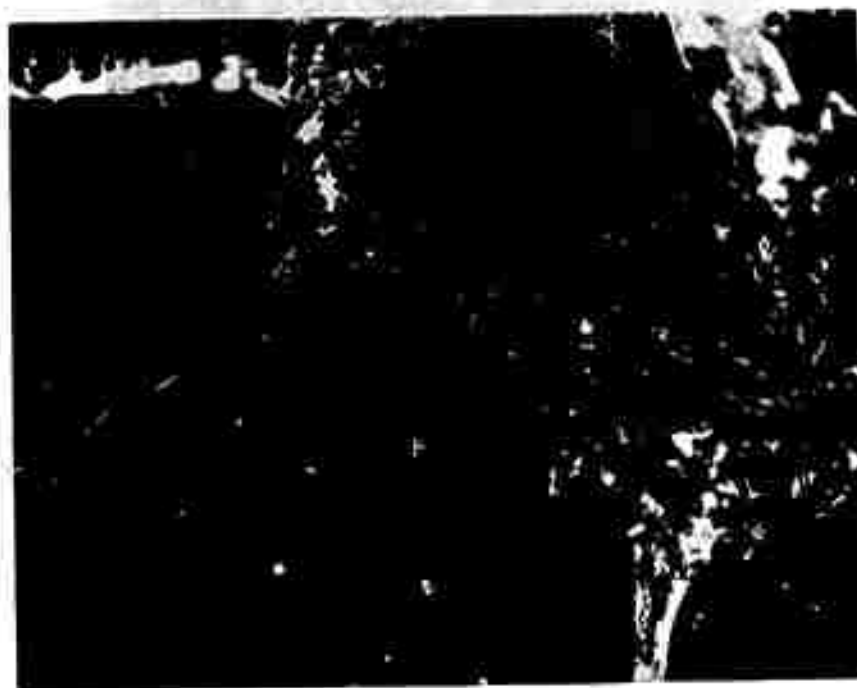


Figure 16. Nd<sub>0.5</sub>Ce<sub>0.5</sub>Co<sub>5</sub> alloy (AR-978) homogenized for 168 hours at 1170°C. Extensive grain growth is evident. Polarized light was employed to reveal the magnetic domain pattern within the large grains.



**Figure 17.** Laue photograph of a  $\text{PrCo}_5$  crystal oriented with its  $c$ -axis parallel to the x-ray beam. The diffraction spots correspond closely with the size and shape of the crystal fragment.

were performed in each case at rates of temperature change of  $\sim 0.5^{\circ}\text{C}$  per minute. At this rate, the points of inflection of the heating and cooling curves generally differed by less than  $1^{\circ}\text{C}$ .

Figure 18 shows the results for the quasi-binary system  $\text{Nd}_{1-x}\text{Ce}_x\text{Co}_5$ . The replacement of neodymium by cerium depresses the Curie temperature slightly faster than one would expect from a linear interpolation between the end points. The results obtained from this series of alloys, which was specifically prepared for this investigation using the same batches of rare earth metals throughout, are nicely consistent. However, significant discrepancies are observed between the  $T_c$  values reported here, particularly that for  $\text{CeCo}_5$ , and what we believe to be the best literature values. In the case of  $\text{CeCo}_5$  we now measure  $T_c = 460^{\circ}\text{C}$ , while an investigation done several years ago by L. Salmans at the Air Force Materials Laboratory<sup>(15)</sup> under the supervision of one of the present authors gave  $T_c = 374^{\circ}$ . Salmans' value was approximately  $50^{\circ}$  and  $90^{\circ}$  lower, respectively, than the two Curie point determinations reported in the literature before the data of his measurement.<sup>(16,17)</sup> In preparing the  $\text{CeCo}_5$  alloy for Salmans (his material was supplied by the University of Dayton) care had been taken to use the purest cerium metal available. Since the Curie point of  $\text{CeCo}_5$  is very much lower than that of any other  $\text{RCo}_5$  (including the immediate neighbors of  $\text{CeCo}_5$ , namely,  $\text{LaCo}_5$  and  $\text{PrCo}_5$ ) the presence of any rare earth impurity in the cerium used would have the effect of increasing the Curie point. Thus, we may attribute the higher

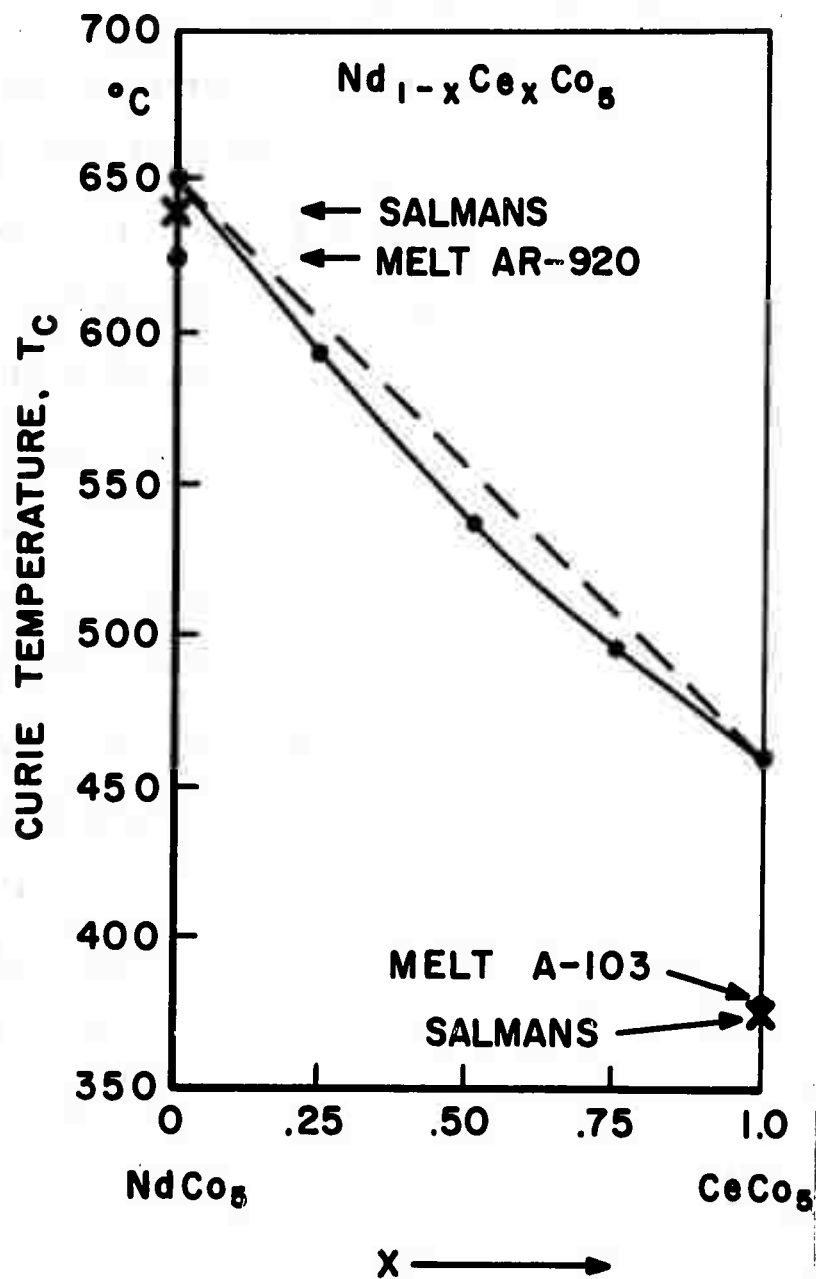


Figure 18. Results of Curie point measurements by TMA in the alloy system Nd<sub>1-x</sub>Ce<sub>x</sub>Co<sub>5</sub>.

T measured now to the presence of relatively large amounts of rare earth impurities, most likely lanthanum, in the cerium metal used in the present investigation.

In interpreting the extraordinarily low value measured by Salmans at the time, we had suggested a different explanation. It is well known that in  $\text{CeCo}_5$  -- as in other cerium compounds -- the magnetic order is strongly enhanced by relatively moderate applied d. c. fields of only several kOe, and therefore the apparent Curie temperature is shifted upward rather strongly by such fields. Since the earlier literature values for  $T_c$  of  $\text{CeCo}_5$  had been derived from magnetization vs. temperature curves measured in d. c. fields on the order of 10 kOe, we had thought that the proper extrapolation to zero field had been neglected and the Curie temperature therefore overestimated. While this may indeed have been the case, this argument cannot be used to explain the high Curie point of  $T_c = 460^\circ\text{C}$  obtained in our present series of measurements, since we used the same technique as Salmans, applying only very small a. c. fields of the order of 1 Oersted.

To shed some light on this puzzle, TMA was performed on a sample of still another  $\text{CeCo}_5$  alloy (A-103) which had been obtained from the Th. Goldschmidt Company in Germany as a raw material for the experimental fabrication of permanent magnets. TMA of this alloy yielded a value of  $T_c = 378^\circ\text{C}$ , in close agreement with the number reported by Salmans and  $80^\circ$  lower than our other value. Apparently the Goldschmidt alloy was prepared from high purity cerium, while the cerium used in the preparation of our own alloy series was contaminated with other rare earth metals.

Unfortunately, it is typical to find this kind of impurity variation in the commercially traded rare earth metals regardless of the purity claims made by the producer.

A similar, although much less severe, discrepancy was found for the  $\text{NdCo}_5$ . In this case, we measured  $T_c = 652^\circ\text{C}$  while Salmans had reported  $640^\circ\text{C}$ . Again, we performed TMA on two other alloys which had previously been prepared at the University of Dayton from neodymium of different

origin. The results were  $T_c = 625^\circ\text{C}$  and  $T_c = 623^\circ\text{C}$ , about  $25^\circ$  lower than

our initial value and somewhat below the value reported by Salmans et al.

Here, it is likely that our present neodymium is of higher purity relative to other rare earths than that used by Salmans or in our own older alloys.

The rare earth impurities most likely to be found in Nd metal are Pr and Ce, and since the 1-5 compounds of both of these have lower Curie points than  $\text{NdCo}_5$ , their presence would tend to depress  $T_c$ .

The results of the Curie point measurements in the system  $\text{NdCo}_5$ - $\text{PrCo}_5$  are shown in Figure 19. Here, we find a value of  $T_c = 619^\circ\text{C}$  for pure  $\text{PrCo}_5$ , compared with  $616^\circ\text{C}$  reported by Salmans and  $620^\circ\text{C}$  measured by us on another older  $\text{PrCo}_5$  alloy which had been prepared from different raw material for a different purpose. These relatively small discrepancies are again attributable to the different impurity content of the rare earth component used. From the rather incomplete data shown in Figure 19 it appears that the substitution of Pr for Nd in  $\text{NdCo}_5$  causes the Curie point to drop fairly rapidly at first so that the measured  $T_c$  values fall substantially

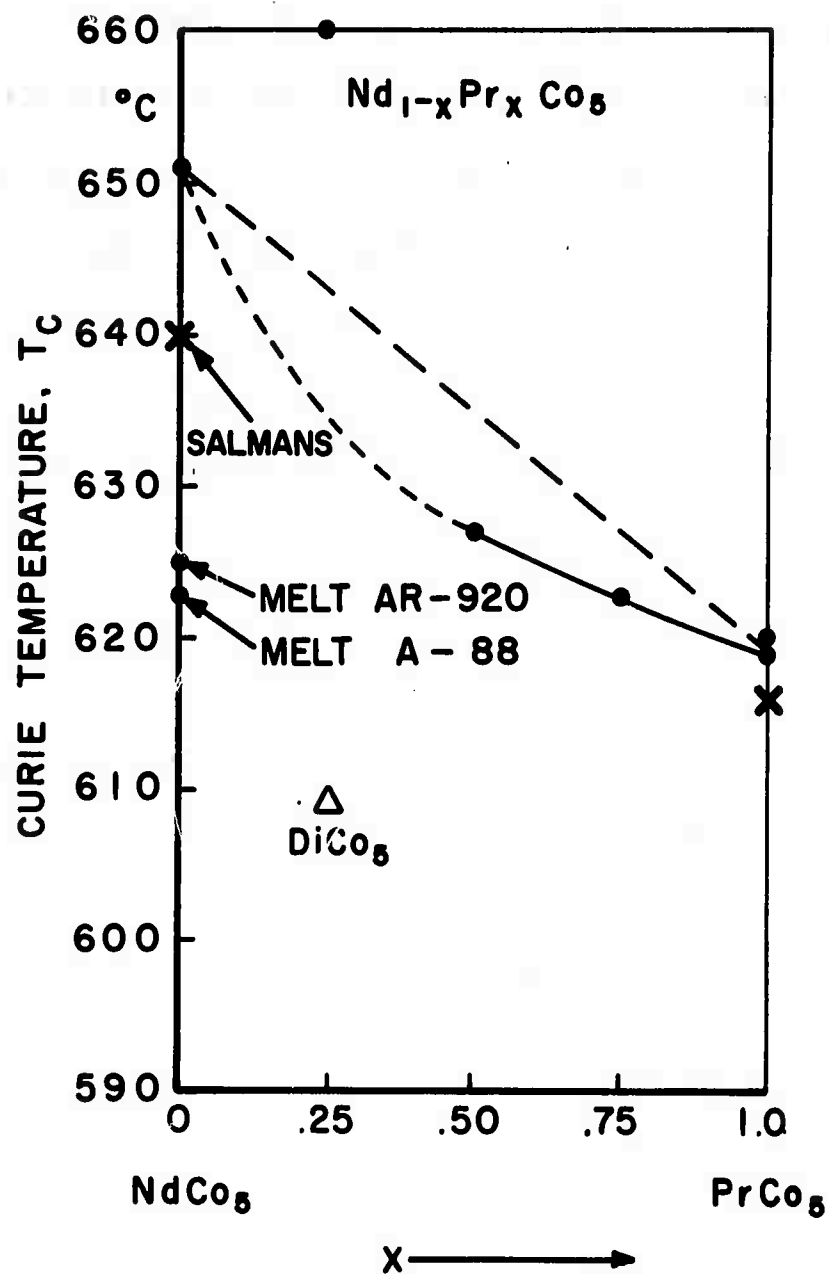


Figure 19. Results of Curie point measurements by TMA in the alloy system  $NdCo_5 - PrCo_5$ .

below the straight line connecting the end points for  $\text{NdCo}_5$  and  $\text{PrCo}_5$ .

However, it must be noted that the point for  $x = 0.25$  is far out of line for reasons unknown. We have to repeat this measurement and fill in points for other values before firm conclusions can be drawn.

Since the commercial rare earth mixture traded under the name didymium (Di) is normally a mixture of 75% Nd and 25% Pr, we decided to make a thermomagnetic analysis on an alloy  $\text{DiCo}_5$  prepared with didymium obtained from the Ronson Metals Corporation. The Curie point of this alloy fell about  $30^\circ$  below the expected value; it was  $T_c = 609^\circ\text{C}$ . This could indicate the presence of substantial amounts of cerium as an impurity in this commercial didymium.

Table V lists all the  $\text{RCO}_5$  alloys on which thermomagnetic analysis was performed, together with the heat treatment each alloy was given before TMA. Where known, the origin of the rare metal used in alloying is identified, and the identification code assigned each alloy at the University of Dayton is also listed to facilitate future cross reference with other measurements which are now in progress and will be reported later.

TABLE V  
LIST OF  $RCO_5$  ALLOYS THERMOMAGNETICALLY ANALYZED

Alloy Code	Alloy Composition	Heat Treatment		Number of TMA Cycles	Peak Temperature Reached in TMA ( $^{\circ}C$ )
		Time (hrs)	Temp. ( $^{\circ}C$ )		
AR-967	$NdCo_5$	168	1225	2	726
AR-979	$(Nd_{.75}Ce_{.25})Co_5$	168	1170	1	647
AR-978	$(Nd_{.5}Ce_{.5})Co_5$	168	1170	1	592
AR-977	$(Nd_{.25}Ce_{.75})Co_5$	168	1170	1	614
AR-976	$CeCo_5$	168	1170	3	569
AR-975	$(Nd_{.75}Pr_{.25})Co_5$	168	1170	2	715
AR-974	$(Nd_{.5}Pr_{.5})Co_5$	168	1170	3	707
AR-973	$(Nd_{.25}Pr_{.75})Co_5$	168	1170	1	664
AR-972	$PrCo_5$	168	1170	1	681
A -200	$DiCo_5$			3	669
A -103	$CeCo_5$			3	835
AR-920	$NdCo_5$	24	1100	1	687
A -88	$NdCo_5$			1	679
AR-659	$PrCo_5$			1	681

### SECTION III

#### METALLURGY OF THE $R_5Co_{19}$ PHASES

##### A. INTRODUCTION

In Technical Report AFML-TR-71-210,<sup>(9)</sup> we reported a new phase in the praseodymium-cobalt alloy system containing between 79 and 80 at.% Co. Prior to his return to the Centre d'Etudes Nucleaires de Grenoble, Dr. J. Schweizer determined that the stoichiometry of this phase is  $Pr_5Co_{19}$  and that it exists in two crystallographic modifications: hexagonal with  $a_{hex} = 5.053 \text{ \AA}$  and  $c_{hex} = 32.47 \text{ \AA}$  and rhombohedral with  $a_{rh} = 5.053 \text{ \AA}$  and  $c_{rh} = 48.71 \text{ \AA}$ . In 1959, Cromer and Larson<sup>(18)</sup> suggested that  $M_5X_{19}$  phases might exist and correctly predicted the crystal structure of these phases.  $Pr_5Co_{19}$  has been associated with the higher of two closely spaced thermal events at  $1124^\circ\text{C}$  and  $1118^\circ\text{C}$  in the Pr-Co phase diagram. Since similar thermal events in the same composition ranges are observed in the Ce-Co and Nd-Co phase diagram,<sup>(19)</sup> it seemed likely that the phases  $Ce_5Co_{19}$  and  $Nd_5Co_{19}$  also exist.

##### B. PREPARATION OF THE ALLOYS (Leasure, Ray)

Three each cerium-cobalt and neodymium-cobalt alloys containing 79.0, 79.5, and 80.0 at.% Co and two praseodymium-cobalt alloys containing 79.2 and 79.5 at.% Co were prepared by arc melting. The stoichiometric amounts of Ce and Nd required were increased by 2 wt.% and the Pr by 1 wt.% to correct for oxygen present in the rare earth metals. All eight

alloys were wrapped in Ta foil and heated at  $1050^{\circ}\text{C}$  for 24 hours. This heat treatment was sufficient to homogenize the Ce-Co and Pr-Co alloys, but the three Nd-Co alloys required an additional 72 hours at  $1100^{\circ}\text{C}$  to achieve homogeneity.

### C. RESULTS (Biermann, Harmer, Kraus, Shanley, Ray)

The lattice constants, Curie temperatures, peritectic temperatures, and metallographic results are given in Table VI. Lattice constant measurements indicate small solubility ranges extending into the Ce-rich and Pr-rich sides of  $\text{Ce}_5\text{Co}_{19}$  and  $\text{Pr}_5\text{Co}_{19}$ , respectively. Evidence concerning a solubility range for  $\text{Nd}_5\text{Co}_{19}$  is inconclusive. The heat treatments given these alloys resulted in stabilizing the rhombohedral form of the  $\text{R}_5\text{Co}_{19}$  phases. In most of the x-ray diffraction patterns, however, a few faint and diffuse lines were observed which could be assigned to the hexagonal form of  $\text{R}_5\text{Co}_{19}$ . It seems likely that  $\text{Ce}_5\text{Co}_{19}$ ,  $\text{Pr}_5\text{Co}_{19}$ , and  $\text{Nd}_5\text{Co}_{19}$  exhibit the hexagonal form only at temperatures very close to the peritectic decomposition temperatures and that the rhombohedral form is stable at lower temperatures. The x-ray powder patterns for the three  $\text{R}_5\text{Co}_{19}$  phases are listed in Table VII.

TABLE VI  
LATTICE CONSTANTS, CURIE TEMPERATURES, AND PERITECTIC TEMPERATURES  
FOR  $\text{Ce}_5\text{Co}_{19}$ ,  $\text{Pr}_5\text{Co}_{19}$ , AND  $\text{Nd}_5\text{Co}_{19}$

Alloy No.	Nominal Composition at. %	Lattice Constants		Curie Temperature ( $^{\circ}\text{C}$ )	Peritectic Temperature ( $^{\circ}\text{C}$ )	Metallography <sup>a</sup>
		a, Å	c, Å			
AR-956	21.0 Ce-79.0 Co	4.943±1	48.77±3	not observed	1129 ±5	$\text{Ce}_5\text{Co}_{19}$ + ~1% $\text{Ce}_2\text{Co}_7$
AR-957	20.5 Ce-79.5 Co	4.938±1	48.69±2	not observed	1130 ±5	$\text{Ce}_5\text{Co}_{19}$ + ~1% $\text{CeCo}_5$
AR-958	20.0 Ce-80.0 Co	4.938±1	48.68±2	not observed	1131 ±5	$\text{Ce}_5\text{Co}_{19}$ + ~15% $\text{CeCo}_5$
AR-936	20.8 Pr-79.2 Co	5.059±1	48.73±1	422 ±5	1125 ±5	$\text{Pr}_5\text{Co}_{19}$ + ~5% $\text{Pr}_2\text{Co}_7$
AR-937	20.5 Pr-79.5 Co	5.054±1	48.73±1	423 ±5	1124 ±5	$\text{Pr}_5\text{Co}_{19}$ + ~1% $\text{PrCo}_5$
AR-953	21.0 Nd-79.0 Co	5.054±1	48.66±3	443 ±5	1156 ±5 <sup>b</sup>	Single phase $\text{Nd}_5\text{Co}_{19}$
AR-954	20.5 Nd-79.5 Co	5.054±1	48.68±3	449 ±5	1155 ±5 <sup>b</sup>	$\text{Nd}_5\text{Co}_{19}$ + ~5% $\text{NdCo}_5$
AR-955	20.0 Nd-80.0 Co	5.054±1	48.65±2	443 ±5	1155 ±5 <sup>b</sup>	$\text{Nd}_5\text{Co}_{19}$ + ~20% $\text{NdCo}_5$

a. All alloys homogenized 24 hours at 1050 $^{\circ}\text{C}$ . The Nd-Co alloys were homogenized an additional 72 hours at 1100 $^{\circ}\text{C}$ .

b. The Nd-Co alloys were made with Nd obtained from Research Chemicals. Similar alloys made with Lunex Nd show the  $\text{Nd}_5\text{Co}_{19}$  peritectic temperature between 1165 and 1170 $^{\circ}\text{C}$ .

TABLE VII  
POWDER X-RAY DIFFRACTION PATTERNS FOR  
 $\text{Ce}_5\text{Co}_{19}$ ,  $\text{Pr}_5\text{Co}_{19}$ , AND  $\text{Nd}_5\text{Co}_{19}$   
(V-Filtered  $\text{Cr K}_\alpha$  Radiation)

hkl	$\text{Ce}_5\text{Co}_{19}$		$\text{Pr}_5\text{Co}_{19}$		$\text{Nd}_5\text{Co}_{19}$	
	Int	d, Å	Int	d, Å	Int	d, Å
0,0,12	VW	4.062	---	-----	W	4.072
0,0,15	VW	3.249	---	-----	--	-----
1,0,13	M	2.816	W	2.846	W	2.847
1,0,14	M	2.701	W	2.726	W	2.729
110	S	2.472	M	2.521	M	2.531
201	S	2.137	M	2.181	M	2.181
1,1,12	S	2.111	S	2.145	S	2.146
0,0,24	S	2.028	M	2.030	M	2.037
1,1,15	M	1.965	W	1.993	W	1.993
2,0,11	M	1.927	---	-----	VW	1.961
1,0,23	W	1.898	VW	1.909	VW	1.910
0,0,27	W	1.8027	W	1.8096	W	1.8050
1,1,24	VW	1.5675	W	1.5828	W	1.5824
2,1,13	W	1.4829	---	-----	W	1.5137
2,1,14	W	1.4688	---	-----	W	1.4947
1,1,27	M	1.4567	W	1.4698	M	1.4675
300	M	1.4266	M	1.4596	M	1.4601
2,0,25	W	1.4400	---	-----	W	1.4536
2,0,26	W	1.4092	VW	1.4236	W	1.4227
3,0,12	VS	1.3452	S	1.3736	M	1.3728
220	S	1.2348	S	1.2635	M	1.2638
1,1,36	---	-----	M <sup>d</sup>	1.1933	M <sup>d</sup>	1.1913

## REFERENCES

1. W. Ostertag and K. J. Strnat, "Rare Earth-Cobalt Compounds with the  $A_2B_{17}$  Structure", Acta Cryst., Vol. 21, 1966, pp. 560-565.
2. K. J. Strnat, G. Hoffer, W. Ostertag and J. C. Olson, "Ferrimagnetism of the Rare Earth-Cobalt Intermetallic Compounds  $R_2Co_{17}$ ", J. Appl. Physics, Vol. 37, 1966, pp. 1252-1253.
3. G. Hoffer and K. Strnat, "Magnetocrystalline Anisotropy of  $YCo_5$  and  $Y_2Co_{17}$ ", IEEE Trans. Magnetics, Vol. MAG-2, 1966, pp. 487-489.
4. G. Hoffer and K. Strnat, "Magnetocrystalline Anisotropy of Two Yttrium-Cobalt Compounds", J. Appl. Physics, Vol. 38, 1967, pp. 1377-1378.
5. K. J. Strnat, "Rare Earth-Cobalt Permanent Magnets," Proceedings of Seventh Rare Earth Research Conference, Coronado, California, Vol. I, 1968, pp. 17-28 (J. F. Nachman, Editor).
6. A. E. Ray, "Iron-Rare Earth Intermediate Phases", Proceedings of Seventh Rare Earth Research Conference, Coronado, California, Vol. II, 1968, pp. 473-484 (J. F. Nachman, Editor).
7. K. Strnat, G. Hoffer and A. E. Ray, "Magnetic Properties of Rare Earth-Iron Intermetallic Compounds", IEEE Trans. Magnetics, Vol. MAG-2, 1966, pp. 489-493.
8. J. Schweizer and J. B. Y. Tsui, University of Dayton, Ohio. See: K. J. Strnat, "Current Problems and Trends in Permanent Magnet Materials", Proceedings 17th Conference on Magnetism and Magnetic Materials, Chicago, Illinois. To be published in AIP Conference Proceeding Series, 1972. Also see Monthly Status Report No. 8, February, 1971, Contract F33615-70-C-1625.
9. A. E. Ray and K. J. Strnat, AFML-TR-71-210, "Research and Development of Rare Earth-Transition Metal Alloys as Permanent Magnet Materials", ARPA Order 1617, USAF Materials Laboratory, Wright-Patterson Air Force Base, Ohio, October, 1971.
10. J. C. Olson, unpublished results, USAF Materials Laboratory, 1965, (See Reference 2).
11. J. Schweizer, unpublished results, University of Dayton, 1971.

12. J. Schweizer, K. J. Strnat and J. B. Y. Tsui, "Coercivity of Heat Treated Pr-Co Powder Compacts", IEEE Trans. Magnetics, Vol. MAG-7, September, 1971, pp. 429-431.
13. A. E. Ray and K. J. Strnat, AFML-TR-71-53, "Research and Development of Rare Earth-Transition Metal Alloys as Permanent Magnet Materials", ARPA Order No. 1617, USAF Materials Laboratory, Wright-Patterson Air Force Base, Ohio, March 1971.
14. R. E. Vogel and C. P. Kempter, "A Mathematical Technique for the Precision Determination of Lattice Parameters", Acta Cryst., Vol. 14, 1961, pp. 1130-1134.
15. L. R. Salmans, K. Strnat and G. I. Hoffer, AFML-TR-68-159, "Magnetic Transition Temperatures of Intermetallic Compounds of Rare Earths with Cobalt and Iron", USAF Materials Laboratory, Wright-Patterson Air Force Base, Ohio, September, 1968.
16. W. E. Wallace and L. V. Cherry, "Studies of Intermetallic Compounds Between the Lanthanide Metals and Fe, Co, Ni and Mn", Rare Earth Research, E. V. Kleber, Editor; McMillan, New York (1961), p. 211.
17. R. Lemaire, "Magnetic Properties of the Intermetallic Compounds of Cobalt with the Rare Earth Metals and Yttrium", Cobalt, No. 32, September, 1966, p. 132, and No. 33, December, 1966, p. 201.
18. D. T. Cromer and A. C. Larson, "The Crystal Structure of  $\text{Ce}_2\text{Ni}_7$ ", Acta Cryst., Vol. 12, 1959, pp. 855-859.
19. A. E. Ray and G. I. Hoffer, "Phase Diagrams for the Ce-Co, Pr-Co and Nd-Co Alloy Systems", Proceedings Eighth Rare Earth Research Conference, Reno, Nevada, Vol. II, 1970, pp. 524-531.